Corroborating the Role of Magnetic Fields and Turbulence in Star Formation via Theoretical Model

Mentor : Mr. Sundar M N
Team MgNaStArS -13
Internship and Projects Division
Society for Space Education Research and Development

July 2021

This project report is submitted in fulfilment of progress requirements for 4-week research internship at SSERD

To all those who seek eternally

Teammates of MgNaStArS -13

- Beno A
- C. Johxy
- Dhrubajyoti Chakraborty
- Kanishk Devgan
- Krishna Bulchandani
- Ninad Khobrekar
- Rahul C V
- Saket Koppineedi
- Soham Sanyashiv
- Soumya Shaw
- Suddhaswattwa Chaudhuri
- Swetha Priya Yanapu

Acknowledgement

At the beginning of this project report, we thank the divine for blessing us in completing this project successfully. We would like to extend our sincere and heartfelt obligation towards Mr. Sujay Sreedhar who is the co-founder and chairman of Society for Space Education Research and Development(SSERD) and Ms. Nikhitha, co-founder and CEO of SSERD for offering us this opportunity to gain research experience in an internship.

Successful completion of any type of project requires help, guidance and support from a number of people. Firstly, we are highly indebted to Mr. Sundar, under whose able guidance and supervision, we were able to actualise our ideas into research work. We would like to thank him for providing us the necessary information and resources for this project. We owe our profound gratitude to Mr. Pavan Kumar for his brainstorming sessions, which helped broaden our perspectives and in avoiding mistakes.

Our heartfelt thanks to Mr. Mahesh for coordinating us throughout the internship. We also would thank Ms. Amaria Bonsi Navis, for helping and providing us support at each and every step of our project making. We wish to express our deep sense of gratitude to each of our team members who have together put in a lot of effort into this project. This undertaking would not have been possible without the support and guidance of a lot of other individuals. And we take this moment to thank the entire SSERD team, our family members, friends and all those who have directly or indirectly helped us during this internship.

Abstract

The team worked upon developing a model (from previous researches) of star formation rate(SFR) dependent on the standard parameters such as β, sonic Mach no. $\mathcal{M}$, turbulence driving parameter b etc. to understand the effects of magnetic fields and turbulence in determining star formation rates. To test the model that was developed using the star formation equation and existing log-normal density PDF relations, we set 2 parameters to run simulations, b and B. We used a 2016 dataset on some star forming giant molecular clouds (SFC GMCs) in Milky Way, choosing the 10 random SFC GMCs from there, and putting their relevant star formation properties in the data. We ran simulations of our model on Python and MATLAB by varying turbulence driving parameter b in the range $[1/3, 1]$, where by previous research and observations, $b \sim (1/3)$ is purely solenoidal and $b \sim 1$ is purely compressive, and the magnetic field B was varied on $[1, 10]\,\mu G$, to see the effect of each on star-formation rates of chosen SFC-GMCs. To study the effect of B on SFR, we fixed the turbulent driving parameter $b \sim 0.4$ i.e. natural mixing of solenoidal and compressive driving modes by previous studies, giving us expected as well as unique and unexpected trends. We saw that the effect of b was more dominant in determining SFR, and compressive driving mode contributes to higher SFRs than B. We conclude from our simulations that more data analysis may be needed to make solid conclusion on the effect of B on SFRs.

Key words: GMC, hydrodynamics- ISM, SFC, SFR:star formation rate, magnetic field, turbulence, MHD: magnetohydrodynamics

Table of Contents

List of Figures

1 Introduction

1.1 Motivation

Since ancient times, we have been fascinated with the heavenly bodies, especially stars, their working and significance in the universe. Star formation, being at the nexus of galaxy formation, planetary science and stellar evolution , is one of the most important concepts in astrophysics.Even after decades of progress in theoretical and practical data , multiple problems are yet to have their veil pulled off. An important question is the role which magnetic fields play in the process of star formation. There are two major classes of star formation theories which differ in the way magnetic field affects the whole process.

The **strong field models** [1; 2], consists of ambipolar diffusion driving core formation and their gravitational collapse to form protostars with magnetic fields controlling the formation and evolution of the molecular clouds. While **weak field models** [3; 4; 5] downplay the significance of role of magnetic field in star formation and state it is supersonic turbulence instead that controls star formation. And in other theories reagarding star formation, with some recent simulations and theoretical developments both magnetic fields and turbulence seem to play significant roles [6; 7][8; 9; 10].Thus it is an open problem as to what are the main quantitative processes which influence star formation rates majorly and how.

1.2 Aims and Objectives

We do know that magnetic fields influence a molecular cloud's morphology and evolution [11].We also know that turbulence plays a major factor in the formation of stars but its direct effect on final formation rates is yet to be determined.The important question that is yet to answered is that what are the main quantitative outcomes set by magnetic fields in the process of star formation.

In view of approaching this question, we would be studying the effect of magnetic fields and turbulence in a molecular cloud which leads to star formation with the help of simulations using our developed mathematical model. Our objective in this project is to develop a theoretical model using ideal magneto-hydrodynamics(MHD) equations and some previous observational work to investigate links between magnetic field, turbulence and star formation rates. Furthermore, we intend to identify which parameter dominates in star formation.

2 Background & Literature Review

2.1 Ideal Magnetohydrodynamics(MHD) Equations

Magnetohydrodynamics plays a major a role in the formation of stars and the ideal MHD equation is used in simulations too.(follows from Hennebelle and Inutsuka [12] and Spruit [13]). The MHD equations assume that fluids are like perfect conductors and their evolution is described by the Maxwell equations. There are four ideal MHD equations (**in CGS units**) as given:

$$\frac{\partial \rho}{\partial t} + \boldsymbol{\nabla} \cdot (\rho v) = 0 \tag{1}$$

$$\rho \left[\frac{\partial v}{\partial t} + (v.\boldsymbol{\nabla})v \right] = -\boldsymbol{\nabla} P + \frac{(\boldsymbol{\nabla} \times B) \times B}{4\pi} \tag{2}$$

$$\rho \left[\frac{\partial e}{\partial t} + (v.\boldsymbol{\nabla})e \right] = -P(\boldsymbol{\nabla} \cdot v) - \rho \mathcal{L} \tag{3}$$

$$\frac{\partial B}{\partial t} = \boldsymbol{\nabla} \times (v \times B) \tag{4}$$

where $\mathcal{L}$ is the net loss function and describes the radiative heating and cooling of the gas. This can be complemented by a state equation to close this system of equations. A perfect gas is a good assumption for ISM, $P = (\gamma - 1)\rho_\epsilon$ where γ is the adiabatic index of the gas.

Equation (4) is also known as MHD **induction equation** and Equation (1) is known as MHD **continuity equation**

2.2 Alfvén's Theorem

In a perfectly conducting fluid, the magnetic flux is a property of the loop i.e. magnetic flux through any closed loop moving with the fluid is conserved with time.

$$\frac{d\Phi_B}{dt} = 0 \tag{5}$$

Also, known as flux-freezing theorem. The 'frozen-in' nature of magnetic fields is of crucial importance in astrophysics(see example in 4.3.1 and 4.3.2 in Davidson [14]) , where R_m i.e. Magnetic Reynold's number(*will be defined in next section 2.3*), is usually very high.
The equivalence of Alfvén's theorem i.e. Equation (5) with the ideal MHD induction equation i.e. Equation (4) is derived on (Pg 40 of Spruit [13])

2.3 Coupling Navier Stokes Equations with MHD Equations

2.3.1 Basic Navier Stokes Equations

Take f as the force acting on continuum, ϕ is it's potential, and ρ is the density of fluid. Let v be the flow velocity with components (v_x, v_y, v_z) in Cartesian Coordinates and p be pressure and τ as deviatoric stress tensor of order 2

Equation of Continuity

$$\frac{\partial \rho}{\partial t} + \boldsymbol{\nabla} \cdot (\rho \vec{v}) = 0 \quad \text{or} \quad \frac{\partial \rho}{\partial t} + \rho \boldsymbol{\nabla} \cdot \vec{v} = 0 \tag{6}$$

In 3D cartesian form it is

$$\frac{\partial \rho}{\partial t} + \frac{\partial (\rho v_x)}{\partial x} + \frac{\partial (\rho v_y)}{\partial y} + \frac{\partial (\rho v_z)}{\partial z} = 0 \tag{7}$$

For steady state conditions, there is no mass accumulation and the equation of continuity becomes

$$\frac{\partial (\rho v_x)}{\partial x} + \frac{\partial (\rho v_y)}{\partial y} + \frac{\partial (\rho v_z)}{\partial z} = 0 \tag{8}$$

For an incompressible fluid, it has negligible variation in density of fluid, so we get

$$\frac{\partial v_x}{\partial x} + \frac{\partial v_y}{\partial y} + \frac{\partial v_z}{\partial z} = 0 \tag{9}$$

Equation of Momentum

In 3D cartesian form, we can write it as three momentum equations:

$$\rho \left[\frac{\partial v_x}{\partial t} + v_x \frac{\partial v_x}{\partial x} + v_y \frac{\partial v_x}{\partial y} + v_z \frac{\partial v_x)}{\partial z} \right] = \rho f_x - \frac{\partial p}{\partial x} + \frac{\partial \tau_{xx}}{\partial x} + \frac{\partial \tau_{yx}}{\partial y} + \frac{\partial \tau_{zx}}{\partial z} \tag{10}$$

$$\rho \left[\frac{\partial v_y}{\partial t} + v_x \frac{\partial v_y}{\partial x} + v_y \frac{\partial v_y}{\partial y} + v_z \frac{\partial v_y)}{\partial z} \right] = \rho f_y - \frac{\partial p}{\partial y} + \frac{\partial \tau_{xy}}{\partial x} + \frac{\partial \tau_{yy}}{\partial y} + \frac{\partial \tau_{zy}}{\partial z} \tag{11}$$

$$\rho \left[\frac{\partial v_z}{\partial t} + v_x \frac{\partial v_z}{\partial x} + v_y \frac{\partial v_z}{\partial y} + v_z \frac{\partial v_z)}{\partial z} \right] = \rho f_z - \frac{\partial p}{\partial z} + \frac{\partial \tau_{xz}}{\partial x} + \frac{\partial \tau_{yz}}{\partial y} + \frac{\partial \tau_{zz}}{\partial z} \tag{12}$$

In index notation, we express the viscous stress tensor

$$\tau_{ij} = 2\mu \, S_{ij} + \lambda S_{mm} \, \delta_{ij} \tag{13}$$

where S_{ij} is the strain rate tensor. μ and λ are the constants to relate viscous stress with strain rate μ is the molecular viscosity coefficient and λ is the bulk viscosity coefficient.
By Stoke's hypothesis, $\lambda = -(2/3)\mu$ which is frequently used, but not yet confirmed. (see 2.6 of Anderson [15])

For an incompressible fluid, Equations (10) - (12) in expanded form for an incompressible fluid can be written as:

$$\rho\left[\frac{\partial v_x}{\partial t}+v_x\frac{\partial v_x}{\partial x}+v_y\frac{\partial v_x}{\partial y}+v_z\frac{\partial v_x}{\partial z}\right]=\rho f_x-\frac{\partial p}{\partial x}+\mu\left[\frac{\partial^2 v_x}{\partial x^2}+\frac{\partial^2 v_x}{\partial y^2}+\frac{\partial^2 v_x}{\partial z^2}\right] \tag{14}$$

$$\rho\left[\frac{\partial v_y}{\partial t}+v_x\frac{\partial v_y}{\partial x}+v_y\frac{\partial v_y}{\partial y}+v_z\frac{\partial v_y}{\partial z}\right]=\rho f_y-\frac{\partial p}{\partial y}+\mu\left[\frac{\partial^2 v_y}{\partial x^2}+\frac{\partial^2 v_y}{\partial y^2}+\frac{\partial^2 v_y}{\partial z^2}\right] \tag{15}$$

$$\rho\left[\frac{\partial v_z}{\partial t}+v_x\frac{\partial v_z}{\partial x}+v_y\frac{\partial v_z}{\partial y}+v_z\frac{\partial v_z}{\partial z}\right]=\rho f_z-\frac{\partial p}{\partial z}+\mu\left[\frac{\partial^2 v_z}{\partial x^2}+\frac{\partial^2 v_z}{\partial y^2}+\frac{\partial^2 v_z}{\partial z^2}\right] \tag{16}$$

But the given equations of momentum conservation is too complicated and big, taking into consideration a lot of aspects which are not necessary especially in our study in astrophysics. (Choudhuri [16] in Chapter 3) gives a simplified version by making reasonable assumptions such as incompressibility of fluid, by which we get:

$$\frac{\partial v}{\partial t}+(v.\boldsymbol{\nabla})v=-\frac{1}{\rho}\boldsymbol{\nabla}p+f+\frac{\mu}{\rho}\boldsymbol{\nabla}^2 v \tag{17}$$

Energy Equation (Conservation Form)

The conservation form of energy equation in terms of total energy i.e. $(e+(v^2/2))$, is :

$$\frac{\partial}{\partial t}\left[\rho(e+\frac{v^2}{2})\right]+\boldsymbol{\nabla}\cdot\left[\rho\left(e+\frac{v^2}{2}\vec{v}\right)\right]=p\dot{q}+\boldsymbol{\nabla}\cdot(k\boldsymbol{\nabla}T)-\boldsymbol{\nabla}\cdot(vp)+\sum_{j}^{x,y,z}\sum_{k}^{x,y,z}\frac{\partial(v_j\tau_{jk})}{\partial k} \tag{18}$$

Note that there are many other possible forms of the energy equation; for e.g., the equation can be written in terms of enthalpy h, or total enthalpy i.e. $(h+v^2/2)$. We will not be deriving or mentioning them here. (to see that in detail, please refer these Anderson [17], Liepmann and Roshko [18], Anderson [19])

Similar to the simplification of momentum conservation equation, (Choudhuri [16] in Chapter 3) gives a version of energy conservation equation, which is quite reasonable in our case of astrophysics. It is given as:

$$\rho\left(\frac{\partial e}{\partial t}+v.\boldsymbol{\nabla}e\right)-\boldsymbol{\nabla}\cdot(k\boldsymbol{\nabla}T)+p\boldsymbol{\nabla}\cdot v=0 \tag{19}$$

2.3.2 Coupling Continuity equation and Induction MHD equation

One form of combining MHD induction equation (Equation (6)) and equation of continuity, is **Walén's Equation** which describes the change of the ratio of magnetic flux to mass density with variation of fluid velocity along a field line

$$\frac{d}{dt}\left(\frac{B}{\rho}\right) = \left(\frac{B}{\rho}.\boldsymbol{\nabla}\right) v \tag{20}$$

By coupling induction MHD equation and continuity equation we get

$$f_L = \frac{1}{4\pi}(\boldsymbol{\nabla} \times B) \times B = -\frac{1}{8\pi}\boldsymbol{\nabla} B^2 + \frac{1}{4\pi}(B.\boldsymbol{\nabla})B \tag{21}$$

The first term on the right is the gradient of what is known as the **magnetic pressure** $B^2/8\pi$ (in SI system, it would be $B^2/2\mu$)

The second term describes a force due to the variation of magnetic field strength in the direction of the field that is known as **magnetic curvature force**

The term $(1/4\pi)(B.\boldsymbol{\nabla})B$ (in SI system, it would be $(B.\boldsymbol{\nabla})B/\mu$ represents **magnetic tension** as B^2/μ). The effects of tension in a magnetic field manifest themselves more indirectly, through the curvature of field lines. (for more detail and discussion on same, please see 1.3.2 and 1.3.3 i.e. Pg 14-16 in Spruit [13])

2.4 Magnetic Diffusivity and Magnetic Reynold's Number

$$\eta = \frac{c^2}{4\pi\sigma_c} = \frac{1}{\mu\,\sigma_c} \text{ i.e. } \textbf{magnetic diffusivity}$$

here μ is the permeability of free space (don't be confused by SI and CGS system here, we are working on CGS here, but sometimes expression in SI also given).

$$R_m = \frac{LV}{\eta} = LV\mu\sigma_c \text{ i.e. } \textbf{Magnetic Reynold's number}$$

Magnetic Reynold's number is useful to the relative importance between the advection term and diffusion term for the relative strengths of advection and diffusion. If $R_m \gg 1$, then advection is more important (ideal MHD limit)
If $R_m \ll 1$, then diffusion is more important In most astrophysical problems, $R_m \ggg 1$ is very large due to large dimensions of astrophysical systems. In the theory of accretion disks, although the Reynold's number is high, still viscosity and diffusion plays an important role, and cannot be neglected. (see 5.7 in Choudhuri [16])

An ionized plasma can have a magnetic diffusivity i.e. η of the order known as *Spitzer value* when dominant non-ideal effect in electrical resistance due to Coulomb interactions of electrons with ions and neutrals

$$\eta \sim 10^{12}\, T^{-3/2}\, cm^2 s^{-1} \tag{22}$$

with temperature T in Kelvin (see Pg 71 of Spruit [13])

2.5 Hydromagnetic Waves

It has been known that, a magnetic fluid i.e. compressible, supports three types of waves, out of which, only one is there which resembles sound waves from classical hydrodynamics. This one wave would be our focus here, as some of it's properties.

The derivation below follows from (14.5 of Choudhuri [16] and 1.8 in Spruit [13]).
Consider a simple case, perturbing uniform fluid (initially at rest $v = 0$) with a homogenous magnetic field B, neglecting dissipative effects such as viscosity, electrical resistivity and heat conduction. Take the initial magnetic field B (here in Cartesian coordinates) along the z direction:

$$B = B_0 \, \hat{z} \tag{23}$$

here, B_0 is a non-negative constant. So, y and x coordinates are equivalent, then we can ignore one of them, take x, by restricting our attention to perturbations δs which are independent of x :

$$\delta_x \, \delta s = 0 \tag{24}$$

Let δB, $\delta \rho$ and δp be little perturbations in magnetic field, density and pressure. Taking $B + \delta B$ as magnetic field, $\rho + \delta \rho$ as the density, and $p + \delta p$ as the pressure. We can write the linear equations of motion and induction as:

$$\rho \frac{\partial v}{\partial t} = \boldsymbol{\nabla} \delta p + \frac{1}{4\pi} (\boldsymbol{\nabla} \times \delta B) \times B \tag{25}$$

$$\frac{\partial \delta B}{\partial t} = \boldsymbol{\nabla} \times (v \times B) \text{ (follows from Equation } (4)) \tag{26}$$

Equation of continuity in our case would be (here ρ is constant), using Equation (6))

$$\frac{\partial \delta \, \rho}{\partial t} + \rho v = 0 \tag{27}$$

As we are neglecting heat conduction, assume adiabatic conditions, so

$$\delta p = \left(\frac{\partial p}{\partial \rho} \right)_{ad} \delta \rho = {c_s}^2 \, \delta \rho \tag{28}$$

here the derivative is taken at constant entropy, c_s is the speed with which acoustic waves travel in the absence of the magnetic fields, and ${c_s}^2 = (\gamma p / \rho)$ where $\gamma = (c_p / c_v)$ i.e. ratio of specific heats for an ideal gas.

The components of Equation (25) and (26) are:

$$\rho \frac{\partial v_x}{\partial t} = -\frac{\partial \delta p}{\partial x} + \frac{B}{4\pi} \left(\frac{\partial \delta B_x}{\partial z} - \frac{\partial \delta B_z}{\partial x} \right) , \quad \rho \frac{\partial v_z}{\partial t} = -\frac{\partial \delta p}{\partial z} \tag{29}$$

$$\rho \frac{\partial v_y}{\partial t} = \frac{B}{4\pi} \frac{\partial \delta B_y}{\partial z} \tag{30}$$

$$\frac{\partial \delta B_x}{\partial t} = B \frac{\partial v_x}{\partial z} \ , \ \frac{\partial \delta B_z}{\partial t} = -B \frac{\partial v_x}{\partial x} \tag{31}$$

$$\frac{\partial \delta B_y}{\partial t} = B \delta v_y z \tag{32}$$

Upon solving Equations (25) - (32), one set of solutions we get, is:
$v_x = B_z = \delta B_x = \delta B_z = \delta p = \delta \rho = 0$, here δB_y and v_y would be determined by Equation (30) and (32). These can together be merged to form the wave equation

$$\left(\frac{\partial^2}{\partial t^2} - {v_A}^2 \frac{\partial^2}{\partial z^2} \right) (\delta B_y, v_y) = 0 \tag{33}$$

where v_A is known as **Alfvén's velocity** and the amplitudes of the Equation (33) are related as

$$\frac{\delta |B_y|}{B} = \frac{|v_y|}{v_A} \tag{34}$$

These solutions is known as Alfvén's waves. As we see, wave equation of it includes components in only y and z coordinates, which implies, this wave propagates only in $y - z$ plane.
As the ideal medium is assumed to be homogenous and time-independent, the occuring perturbation can be decomposed as planar waves which can be represented in the usual way in terms of a complex amplitude.
An arbitrary quantity varies with space and time as:

$$q = q_0 \exp\left[i(\omega t - kx)\right] \tag{35}$$

Here time and spatial representation derivatives are replaced by $i\omega$ and $-ik$ respectively, where ω is angular velocity, $q_0 \in \mathbb{C}$ is a constant and $k \in \mathbb{R}$ is the direction of propagation of the wave.
By Equation (35) and (33), we get the basic dispersion relation for Alfvén's waves

$$\omega^2 = {k_z}^2 {v_A}^2 \tag{36}$$

By which, we get

$$\omega = v_A k_z \cos\theta \tag{37}$$

where θ is the angle between magnetic field and propagation vector, here k_z. Note that group velocity i.e. the direction of propagation of wave energy is

$$\frac{\partial \omega}{\partial k} = v_A \hat{z} \tag{38}$$

Since Equation (37) only involves k_z, we can say that Alfvén waves propagate along the magnetic field with frequency depending on just the wave number component along B and displacement being always in transverse direction

As we mentioned just after Equation (21) about magnetic field having a tension i.e. $B^2/4\pi$ associated with it along the field lines. Ideally, a magnetic field in a plasma can be thought to be a stretched string. The magnetic tension tries to oppose any distortion caused by a transverse perturbation. In this case, so take a transverse Alfvén wave moving along the field lines, velocity of such a wave can be given similar to how we express the velocity of a wave moving along a stretched string i.e. $\sqrt{\text{tension}/\text{ density}}$, and so we get an expression of Alfvén's velocity v_A (see 14.5 in [16])

$$v_A = \sqrt{\frac{B^2/4\pi}{\rho}} = \frac{B}{\sqrt{4\pi\rho}} \tag{39}$$

For a more detailed and rigorous derivation of Alfvén's velocity, see [20], and for further discussion on Alfvén waves, see the former and Pg 29 onwards of [13].

2.6 Further Developments upon MHD covered

2.6.1 Sonic, Alfvénic Mach Numbers and Plasma β

While ignoring any external forces acting like gravity we get

$$\rho\frac{dv}{dt} = -\boldsymbol{\nabla}p + \frac{1}{4\pi}(\boldsymbol{\nabla}\times B)\times B \tag{40}$$

Take a characteristic length scale l and time scale $\mathcal{T}$, v_0 for velocity and B_0 for field strength. For the ideal case of transmission of sound wave, assume a compressible medium. For the sake of simplicity take the isothermal equation of state $p = \mathcal{R}\,\rho\,T$ where T is the temperature and $\mathcal{R}$ is the gas constant. Let all dimensionless variables be denoted with an asterix * (follows from Pg 18-19 of [13])

$$t = \mathcal{T}\,t^* \;\;,\;\; \boldsymbol{\nabla} = \frac{\boldsymbol{\nabla}^*}{l} \;\;,\;\; v = v_0\,v^* \;\;,\;\; B = B_0\,B^* \tag{41}$$

Let c_i be the isothermal sound speed

$$c_i{}^2 = \frac{p}{\rho} = \mathcal{R}T \tag{42}$$

Multiplying equation of motion by (l/ρ).Similar to non-dimensionalisation, we did to get Equation (**??**), we proceed as follows:

$$v_0\,\frac{l}{\mathcal{T}}\,\frac{d}{dt^*}v^* = -c_i{}^2\,\boldsymbol{\nabla}^*\ln\rho + v_A{}^2\,(\boldsymbol{\nabla}^*\times B^*)\times B^* \tag{43}$$

The characteristic value for phenomenon occurring at the time scale $\mathcal{T}$ is simply $v_0 = l/\mathcal{T}$. To get a zero-dimension form of the equation of motion, we divide Equation (43) by $c_i{}^2$

$$\mathcal{M}^2\frac{d}{dt^*}v^* = -\boldsymbol{\nabla}^*\ln\rho + \frac{2}{\beta}(\boldsymbol{\nabla}^*\times B^*)\times B^* \tag{44}$$

here $\mathcal{M}_s$ is the **Mach number** of the flow i.e. given by

$$\mathcal{M} = \frac{v_o}{c_i} \tag{45}$$

and β is the **plasma-β** i.e. ratio of gas pressure to magnetic pressure given by

$$\beta = \frac{c_i{}^2}{v_A{}^2} = \frac{8\pi p}{B_0{}^2} \tag{46}$$

Similar, to how we have defined $\mathcal{M}$, we define **Alfvénic Mach Number** $\mathcal{M}_A$ i.e.

$$\mathcal{M}_A = \frac{v_0}{v_A} \tag{47}$$

As l, v_0, $\mathcal{T}$ and B_0 are taken as representative values in the beginning, so the starred quantities(with asterix) defined in Equation (41), are all of order unity.

2.6.2 Cases of β and $\mathcal{M}$ to consider

We would consider here some cases of $\mathcal{M}$ and β which are important to pay attention to (the discussion below follows from [13] and please refer 1.4 in it for more detail)

- $\mathcal{M} \ll 1$: a highly subsonic flow. In this case, the LHS of Equation (44) can be neglected, and β becomes highly important in determining the character of the problem.
- $\beta \gg 1$: by definition of β, in this case, gas pressure $\gg$ magnetic pressure that implies gas pressure $\gg$ magnetic energy density which further implies that the second term in the RHS of Equation (44) is too small. So, the first term in RHS must be small as well, as $\boldsymbol{\nabla}^* \ln \rho \ll 1$, meaning that acting magnetic forces result in extremely small changes in density.In the absence of external field, we can make an approximation for constant density in such kind of high β environments.
- $\beta \ll 1$: by definition of β, gas pressure $\ll$ magnetic pressure, so the second term in RHS of Equation (44) must be large, but due to the presence of logarithm in the first term, it won't be able to balance it out. Therefore, in case of, low β, low $\mathcal{M}$, for magnetic forces to be little, we must have the following condition

  $$(\boldsymbol{\nabla} \times B^*) \times B^* \sim \mathcal{O}(\beta) \ll 1 \tag{48}$$

  for $\beta \to 0$, we have two solutions:

  - vanishing current i.e. $\boldsymbol{\nabla} \times B = 0$: In this case, the field is known as *potential field* as it has a scalar potential, say ϕ_m such that $B = -\boldsymbol{\nabla}\phi_m$ with $\boldsymbol{\nabla} \cdot B = 0 \implies \boldsymbol{\nabla}^2 \phi_m = 0$
  - $\boldsymbol{\nabla} \times B \parallel B$: $(\boldsymbol{\nabla} \times B) \times B = 0$. In general, this case describes *force free fields*. ([13; 21; 22]
- Significant $\mathcal{M}$ and large β : In this case, the second term in RHS of Equation (44) can be neglected, by which we get a classical hydrodynamics scenario with magnetic field playing a passive role.
- Small β but field neither force-free nor potential field : In such a special case, balance can only be attained when $\mathcal{M}$ is of the order of $1/\beta \gg 1$ which implies existence of supersonic flows with velocities $v_0 \sim v_A$. In some theories of star forming molecular clouds such as weak-field models mentioned before ([3; 4; 5]), the magnetic fields are approximated to be in such a regime.
- $\beta \approx 1$: This case is sometimes known as *equipartition* i.e. approximate equality of thermal and magnetic energy densities (follows from definition of β). In some situations, equipartitions also refers to a state where kinetic energy density of flow is comparable to magnetic energy density i.e.

  $$\frac{1}{2}\rho v^2 \approx \frac{B^2}{8\pi} \implies v^2 \approx \frac{B^2}{4\pi\rho} \implies v \approx v_A \tag{49}$$

2.7 Virial theorem and Beyond

Virial theorem is quite an important theorem as by using it, we can analyze the relative importance of magnetic fields with respect to self-gravity, turbulent ram pressure and thermal pressure of molecular clouds.

In Eulerian form, virial theorem can be written like as below i.e. Equation (50) for a fixed volume. This builds up from the Lagrangian form of virial theorem for a fixed mass. ([23; 24], [25])
Take a fixed control volume V, containing fluid with density ρ, having velocity v, it's magnetic field as B and gravitational potential as ϕ, is given by ([26]) as follows:

$$\frac{1}{2}\ddot{I} = 2(\mathcal{T} - \mathcal{T}_0) + (\mathcal{B} - \mathcal{B}_0) + \mathcal{W} - \frac{1}{2}\frac{d}{dt}\int_{\delta V} (\rho v r^2)\, dS \tag{50}$$

(follows from the explanation in Krumholz and Federrath [27], McKee and Ostriker [4]) here, $\ddot{I}$ is the second derivative of the generalized moment of inertia of the mass within V
$\mathcal{T} = \frac{1}{2}\int (3P + \rho v^2)\, dV$ is the total translational thermal plus kinetic energy.

$\mathcal{B} = \frac{1}{8\pi}\int B^2 dV$ is the total magnetic energy

$\mathcal{W} = -\int \rho r \cdot \boldsymbol{\nabla}\phi\, dV$ is the gravitational potential energy
$\mathcal{T}_0$ and $\mathcal{B}_0$ are fluid and magnetic stresses respectively about the surface of V

The RHS of the equation (50) describes how the forces acting on V cause the material inside the volume to accelerating inbound or outbond direction.
Take ratios of force terms on RHS of Equation (50) in order to yield zero-dimension ratios gives numbers which describe their relative importance. Furthermore, take the ratio of magnetic to two parts of kinetic term, we get (from [27])

$$\frac{\mathcal{B}}{(3/2)\int P\, dV} \sim \frac{B^2/8\pi}{P} \sim \beta^{-1} \tag{51}$$

$$\frac{\mathcal{B}}{(1/2)\int \rho v^2\, dV} \sim \frac{B^2/8\pi}{\rho v^2} \sim (\frac{v_A}{v})^2 \sim \mathcal{M}_A^{-2} \tag{52}$$

$$\text{where} \qquad v_A = \frac{B}{\sqrt{4\pi\rho}} \quad \text{i.e. } \textbf{Alfvén velocity} \tag{53}$$

here, β is the **plasma parameter(or efficiency parameter)** defined in Equation (46) and $\mathcal{M}_A$ is **Alfvén Mach number**, defined in Equation (47)

Assuming that the external fields are negligible compared to the volume's self gravity,
so $\mathcal{W} \sim -GM^2/R$
For a uniform spherical volume, assuming the condition of negligibility other force fields compared to self gravity, $\mathcal{W} = -\frac{3}{5}\frac{GM^2}{R}$ would be the gravitational energy of a uniform sphere with an extra factor a to account for deviations in shape and density distribution. (see [28])
So, for an arbitrary volume V, take the ratio of magnetic and gravitational terms, we get(follows from [27])

$$\frac{\mathcal{B}}{\mathcal{W}} \sim \frac{(B^2R^3)/8\pi}{GM^2/R} \tag{54}$$

here M is the mass contained in volume and $R = V^{1/3}$ is the characteristic size. In ideal MHD, the magnetic flux through the volume is conserved by Alfvén's Theorem ((5)), so the ratio can be re-written in terms of magnetic flux as $\Phi_B \sim BR^2$ and so

$$\frac{\mathcal{B}}{\mathcal{W}} \sim \frac{\Phi_B^2}{GM^2} \sim \mu_\Phi^2 \tag{55}$$

$$\text{where} \quad M_\Phi = \frac{1}{2\pi}\frac{\Phi_B}{\sqrt{G}} \quad \text{i.e. } \textbf{magnetic critical mass} \tag{56}$$

M_Φ is the magnetic critical mass which is the maximum mass that can be supported from collapse by a specified magnetic flux or gravitational collapse([29])
Note that the exact coefficient in M_Φ depends weakly on the configuration of the mass; the value $1/2\pi$ that we have adopted in Equation (56) is by assuming an infinite thin sheet ([30])
The relative importance of magnetic field in supporting a cloud against gravitational collapse is usually quantified by the mass to flux ratio i.e. $\mu_\Phi = M/M_\Phi$
For a cold cloud in equilibrium,(see [28])

$$M = c_\Phi \frac{\Phi_B}{G^{1/2}} \tag{57}$$

If we take the simplest case for a uniform poloidal field through a spherical cloud $\Phi_B = \pi R^2 B$
In the Equation (57), c_Φ is a constant of order unity which depends on the distribution of magnetic fields and density within the cloud. A cold cloud with a constant mass to flux ratio poloidal field has $c_\Phi \approx 0.17$ ([31])
If $\mu_\Phi > 1$, the cloud is called *supercritical* and the magnetic field cannot prevent gravitational collapse of a cloud on it's own. However, if $\mu_\Phi < 1$ then the cloud is said to be *subcritical*, and gravitational collapse of this cloud is not possible. Based on classical star formation theories(such as [32]), for a subcritical core to be able to collapse, either the mass must change (such as from flows along field lines), or μ_Φ must change via **ambipolar diffusion**(which results from magnetic field lines in dense regions not being perfectly frozen to the gas).

Points to note : We have implicitly assumed μ_Φ to be constant, which is only true when the flux is conserved, that holds for ideal MHD, but non-ideal effects do play a major role at some point in the star formation process, as evidenced by the fact that magnetic fields of young stars are more weaker than in the situation where all the magnetic flux which threads a typical $\sim 1M_\odot$ interstellar cloud were to be trapped into the star when it collapses(such as e.g. [33]).
At largest scales, non-ideal mechanism(ambipolar diffusion) operates. As per ([34]), observed molecular clumps are seen to have $R_{AD} \approx 20$ that places them near but not exactly close to the ideal MHD limit (*i.e.* $R_{AD} \to \infty$. So, we would be assuming ideal MHD here. Although, we to have to keep in mind, that if non-ideal effect are added where relevant, then the model might be more realistic and accurate.

2.8 Stability and Collapse of Gas Cloud

2.8.1 Jeans Instability and Criterion

Consider an infinite, uniform, homogenous gas cloud at rest with density ρ, pressure p and temperature T, both of which are constant everywhere. Note that this state is not a well-defined equilibrium.(chapter 7 of [16], chapter 26 of [35], chapter 8 of [36] and [37]).
We would be investigating under which circumstances, such a configuration can become unstable due to self-gravity. The gas cloud is described by the Navier Stokes equation of continuity and motion.(*here we would be neglecting viscosity*)

$$\frac{\partial \rho}{\partial t} + \boldsymbol{\nabla} \cdot (\rho v) = 0 \tag{58}$$

$$\frac{\partial v}{\partial t} + (v.\boldsymbol{\nabla})v = -\frac{1}{\rho}\boldsymbol{\nabla} p - \boldsymbol{\nabla}\Phi \tag{59}$$

By Poisson's equation,

$$\boldsymbol{\nabla}^2\Phi = 4\pi G\rho \tag{60}$$

where G is the Newtonian gravitational constant, k_B is the Boltzmann constant, μ is the mean molecular weight and m is the mass of gas particles
Assume the gas is isothermal, and so we have the equation of state

$$p = \frac{\mathcal{R}}{\mu}\rho T = \frac{(k_B/m)}{\mu}\rho T = {c_s}^2\rho \tag{61}$$

This assumption is justified as energy exchange by radiation is usually quite efficient for interstellar matter which means the time scales for thermal adjustment are short compared to the dynamical processes being studied here.
Take constant ρ_0 as initial density, p_0 as the initial pressure for the gas. For equilibrium, let $\rho = \rho_0 =$ constant , $T = T_0 =$ constant, and $v_0 = 0$. ϕ_0 is determined by $\boldsymbol{\nabla}^2\Phi_0 = 4\pi G\rho_0$ and by boundary conditions at infinity Here, we would consider a small perturbation, as below:

$$\rho = \rho_0 + \rho_1 \ , \ p = p_0 + p_1 \ , \ \Phi = \Phi_0 + \Phi_1 \ , \ v = v_1 \tag{62}$$

Here, the functions with subscript 1 depend on space and time.
The perturbation of equation of continuity gives:

$$\frac{\partial \rho_1}{\partial t} + \rho_0\boldsymbol{\nabla} \cdot v_1 = 0 \tag{63}$$

Linearizing Equation (62) and substituting in (59) and (61), assuming the perturbations are isothermal(c_s *is not perturbed*) and ignoring non-linear quantities, we get

$$\rho_0\frac{\partial v_1}{\partial t} = -{c_s}^2\boldsymbol{\nabla}\rho_1 - \rho_0\boldsymbol{\nabla}\Phi_1 \tag{64}$$

$$\boldsymbol{\nabla}^2\Phi_1 = 4\pi G\rho_1 \tag{65}$$

We have now three equations (63), (64) and (65), satisfied by the three perturbation variables ρ_1, v_1 and Φ_1. This is a system of linear homogeneous system of differential equations with constant

coefficients. We therefore can assume that solutions exist with the space and time dependence proportional to $\exp[i(kx+\omega t)]$ such that:

$$\frac{\partial}{\partial x} = ik \ , \ \frac{\partial}{\partial y} = \frac{\partial}{\partial z} = 0 \ , \ \frac{\partial}{\partial t} = i\omega \tag{66}$$

and we obtain

$$\omega v_1 + \frac{k{c_s}^2}{\rho_0}\rho_1 + k\Phi_1 = 0 \tag{67}$$

$$k\rho_0 v_1 + \omega\rho_1 = 0 \tag{68}$$

$$4\pi G\rho_1 + k^2\Phi_1 = 0 \tag{69}$$

The set of equations above (67)- (69) can only have non-trivial solutions if

$$\begin{vmatrix} \omega & (k{c_s}^2/\rho_0) & k \\ k\rho_0 & \omega & 0 \\ 0 & 4\pi G & k^2 \end{vmatrix} = 0 \tag{70}$$

i.e. if

$$\omega^2 = k^2{c_s}^2 - 4\pi G\rho_0 \tag{71}$$

where k is a non-vanishing wave number. There exist two different cases:

- if k is sufficiently large then $k^2{c_s}^2 - 4\pi G\rho_0 > 0$ and $\omega \in \mathbb{R}$. The perturbation varies periodically in time and equilibrium is stable with respect to perturbations of such short wavelengths.
  In the case, of limit $k \to \infty$ in Equation (71), we get $\omega^2 = k^2{c_s}^2$ which corresponds to isothermal sound waves.
- if $k^2{c_s}^2 - 4\pi G\rho_0 < 0$ then ω is of the form $i\xi$ where $\xi \in \mathbb{R}$. So, perturbations $\sim \exp(\xi t)$ which grow exponentially with time i.e. unstable equilibrium.

The intermediate between these two cases corresponds the critical wave number

$$k_J = \left(\frac{4\pi G\rho_0}{{c_s}^2}\right)^{(1/2)} \tag{72}$$

or to the critical wavelength

$$\lambda_J = \frac{2\pi}{k_J} = \left(\frac{\pi}{G\rho_0}\right)^{(1/2)} c_s \tag{73}$$

Therefore, a perturbation with a wave number $k < k_J$ (or a wavelength $\lambda > \lambda_J$) is unstable.

The condition for instability $\lambda > \lambda_J$ is known as **Jeans Criterion**.
The corresponding critical which is often referred as **Jeans Mass** is given by (using Equation (61) in second part)

$$M_J \ = \ \frac{4}{3}\pi{\lambda_J}^3\rho_0 \ = \ \frac{4}{3}\pi^{5/2}\left(\frac{k_B T_0}{Gm}\right)^{3/2}\frac{1}{\rho^{1/2}} \tag{74}$$

So, $M_J \propto {T_0}^{3/2}\,{\rho_0}^{-1/2}$ If the perturbation in a uniform gas cloud with temperature T_0 and density ρ_0, involves $M > M_J$ then it can be said that gas in the perturbed region would keep contracting due to the enhanced self gravity eventually fragmenting into pieces due to Jean's instability.

A cloud which exceeds Jeans Mass collapses and undergoes *fragmentation*. The collapse is assumed to be isothermal more than adiabatic. As, cloud falls together and fragments of it become unstable and collapse faster than the cloud as a whole, Jeans mass becomes smaller than the mass of the parent collapsing cloud. This process goes on until the collapse remains isothermal. (Note: The concept of Jeans Mass is derived for an equilibrium state, but for estimation purposes at the order-of-magnitudem we can use it).
A detailed estimate, considering radiation processes was given by [38] and another by [39] who gave an estimate of the mass limit of fragmentation without specifying the detailed radiation process. To see more detail upon how this fragmentation eventually leads to star formation, see Chapter 27 of [35], [36], [40], [41])

2.8.2 Free-Fall Time for Homogeneous Cloud Collapse

Jeans Criterion follows from an ordinary first-order perturbation theory by which we obtain conditions under which perturbations of equilibrium stange tend to develop exponentially. But this does not give enough information about a fully developed collapse and the final product. In order to know that, the next step taken is to study this process through non-linear perturbations. Here, we begin with the simplified case i.e. of spherically symmetrical cloud. The derivation and explanation below follows from (chapter 27 of [35], chapter 8 of [36] and [37])

Consider a spherically symmetrical, homogeneous collapsing cloud having mass M, radius R, assuming free-fall i.e. the forces due to pressure gradients would be neglected. As, the gravitational force for sphere $\sim -GM\ R^2$, pressure term in the equation of motion can be approximated by

$$\left|\frac{1}{\rho}\frac{\partial P}{\partial R}\right| \approx \frac{P}{\rho R} \approx \frac{\mathcal{R}T}{\mu\, R} \tag{75}$$

The ratio of gravitation to pressure term $\propto M/(RT)$, which during isothermal collapse increases as R decreases. (*M is const.*). Since, we are neglecting pressure, the sphere collapses in free-fall, by the equation of motion

$$\ddot{r} = -\frac{Gm}{r^2} \tag{76}$$

here, we can take $m = (4/3)\pi {r_0}^3 \rho_0$ where r_0 and ρ_0 are the initial values of radius and mass of sphere at the beginning of collapse, let $\rho_0 =$ const. Multiplying, Equation (76) by $\dot{r}$ and integrating it, we get

$$\frac{1}{2}\dot{r}^2 = \frac{4\pi {r_0}^3}{3r} G\rho_0 + C \tag{77}$$

Take the integration const C such that $dotr = 0$ at the beginning, when $r = r_0$, so we obtain

$$\frac{\dot{r}}{r_0} = \pm\sqrt{\frac{8\pi G}{3}\rho_0 \left(\frac{r_0}{r} - 1\right)} \tag{78}$$

for $r \in \mathbb{R}$, $r < r_0$ i.e. only the negative sign of the RHS of this equation gives relevant solutions. Take a variable θ defined as

$$\cos^2\theta = \frac{r}{r_0} \tag{79}$$

So,

$$\frac{\dot{r}}{r_0} = -2\dot{\theta}\cos\theta\sin\theta\ ,\ \ \frac{r_0}{\dot{r}} - 1 = \frac{\sin^2\theta}{\cos^2\theta} = \tan^2\theta \tag{80}$$

Using Equation (78)

$$2\dot{\theta}\cos^2\theta = \sqrt{\frac{8\pi G\rho_0}{3}} \tag{81}$$

By basic trigonometry, we can derive the following identity

$$2\dot{\theta}\cos^2\theta = \frac{d}{dt}\left(\theta + \frac{1}{2}\sin 2\theta\right) \tag{82}$$

Using this identity, in our equation, we get

$$\theta + \frac{1}{2}\sin 2\theta = t\sqrt{\frac{8\pi G\rho_0}{3}} \tag{83}$$

where the integration const C is chosen such that the beginning of the collapse (i.e. when $r = r_0$ or $\theta = 0$) coincides with $t = 0$. Note that, r_0 is absent in the equation (83). So, the solution $\theta(t)$ can be used for all mass shells. Similarly, r/r_0 and $\dot{r}/r_0$ at a given time t in Equation (80) is also valid for all mass shell. This implies that the sphere undergoes a *homologous contraction*. So, the relative density variation doesn't depend on the r_0 and the sphere at all. The time it would take to reach the centre ($r = 0$ or $\theta = \pi/2$) is known as **free-fall time**

$$t_{\text{ff}} = \sqrt{\frac{3\pi}{32\,G\rho_0}} \tag{84}$$

which follows from Equation (83) and is applicable to all mass shells. Keep in mind that, before the centre is reached, the pressure will become relevant as the gas becomes opaque and T increases. In that situation, the free-fall approximation has to be abandoned and finally the collapse would terminate. (see 27.2 - 27.5 of [35] for more detail)

The sound travel time across the cloud is given by (using equation (94) too)

$$t_s = \frac{R}{c_s} = R\sqrt{\frac{\rho}{p}} = R\sqrt{\frac{\mu}{\mathcal{R}T}} \tag{85}$$

When $t_s < t_{\text{ff}}$, pressure forces overcome gravity temporarily, returning the system to stable equilibrium. While, when $t_s > t_{\text{ff}}$ gravity is able to overcome pressure forces leading to gravitational collapse of cloud. So, a condition of collapse

$$t_s \geq t_{\text{ff}} \tag{86}$$

Using Equation (86), we can get the condition of critical Jeans Mass again and Jeans Instability.

The view of star formation presented here is extremely simplified, neglecting important effects such as magnetic field, cloud rotation and turbulence. Any collapsing cloud having zero angular momentum is highly unlikely . In the absence of a braking torque, cloud's rotational velocity increases because angular momentum is conserved during gravitational collapse. If the magnetic field is connected to surrounding gas, the necessary braking torque maybe produced. These are crucial points to keep in mind when dealing with star formation. (see 8.1.4 in [36]).
As we move on, the star formation processes would become more realistic than it is now, as we would be taking both magnetic fields and turbulence driving parameter into consideration as well.

2.9 Playing with Turbulence and Magnetic Fields

2.9.1 Introduction

Turbulence can be found to play a dominant role almost everywhere throughout the Milky Way, especially in galactic processes like star formation ([42], [43], [4] , [44]). Being such an immense topic in astrophysics, our discussion of turbulence is just a brief review and would be taking help from variety of exhaustive reviews on the subject such as [45], [46], [47], [43], [48]

Based on the previous background review, the dynamic nature of MHD flow can be characterized by two non-dimensional parameters fully

$$R_e{}^{-1} = \frac{\mu}{Lv} \ , \ R_m{}^{-1} = \frac{\eta}{Lv} \tag{87}$$

where R_e is the kinetic Reynold's number(of ordinary hydrodynamics) with viscosity μ and R_m is the Magnetic reynold's number with η as the magnetic diffusivity. In the case, R_e and R_m become sufficiently larger than unity, the MHD flow undergoes a transition from the laminar state (*stationary stream-line topology*) to turbulence in which the fluid motion seems to become erratic and unpredictable. ([47])
Although our understanding about the working of turbulence is surprising little but there have been many simple models and tools that describe it, some of those which would be mentioned here.

2.9.2 Velocity Statistics

Velocity fluctuates in space and time in a turbulent medium, making the statistical approach a reasonable way to proceed with the study of such fluctuations. Astrophysics employs a lot of statistical tools, but here we would be discussing some of the simpler ones, and make two assumptions which simplify our work that are assuming homogeniety and isotropic nature of turbulence. In a real molecular cloud, both of these assumptions aren't strictly true as huge magnetic fields provide a preferred direction, so the isotropic condition is an ideal case. But as we move on, we can build up from these and relax those assumptions. (the explanation and derivation follows from [49])

Take $v(x)$ as the velocity at position x within volume V. The autocorrelation function which describes how it varies with position is given by

$$A(r) = \frac{1}{V}\int v(x)\cdot v(x+r) \equiv \langle\, v(x)\cdot v(x+r)\,\rangle \tag{88}$$

where the angle brackets denote the average over all positions x. $A(0) = \langle |v|^2 \rangle$ is the mean square velocity in the fluid. If the velocity is taken to be isotropic, then we see, $A(r)$ doesn't depend on direction, but only on $r = |r|$. So, by $A(r)$, we can tell the relative difference between the velocities at points separated by some distance r. This can be thought of in a better way in Fourier space than in a real space, so the autocorrelation resembles a Fourier transform. The Fourier transform of the velocity field is

$$v(k) = \frac{1}{(2\pi)^{3/2}}\int v(x)\, e^{-ikx}\, dx \tag{89}$$

The power spectrum is defined as

$$\Psi(k) = |\tilde{v}(k)|^2 \tag{90}$$

As turbulence is taken to be isotropic, the power spectrum depends only on the magnitude of the wave number, $k = |k|$, and not on it's direction, so it is usual to define the power per unit radius in k-space

$$P(k) = 4\pi k^2 \Psi(k) \tag{91}$$

where this is the total power integrated over some shell from k to $k + dk$ in k-space. By Parseval's theorem, we have

$$\int P(k)\, dk = \int |\tilde{v}(k)|^2\, dk = \int v(x)^2\, dx \tag{92}$$

i.e. the integral of power spectral density over all wavenumbers which is equal to the integral of the square of the velocity over all space. For an incompressible flow, the integral of power spectrum gives the kinetic energy per unit mass in the flow. By Weiner-Khinchin theorem , $P(k)$ is just the Fourier transform of the autocorrelation function ([50])

$$\Psi(k) = \frac{1}{(2\pi)^{3/2}} \int A(r)\, e^{-ikr}\, dr \tag{93}$$

Consider a volume of size l and measure the velocity dispersion within it. Furthermore, suppose the power spectrum is described the power law $P(k) \propto k^{-n}$ then the kinetic energy per unit mass within the region is upto factors of order unity,

$$KE = \sigma_v(l)^2 \tag{94}$$

another way of expressing KE is in terms of power spectrum, integrating over the modes that are small enough to fit within the volume under consideration

$$KE \sim \int_{2\pi/l}^{\infty} P(k) dk \propto l^{n-1} \tag{95}$$

Using which, we get

$$\sigma_v = c_s \left(\frac{l}{l_s}\right)^{(n-1)/2} \tag{96}$$

where the relationship is normalized by defining sonic scale l_s as the size of a region within which the velocity dispersion is equal to the thermal sound speed of gas i.e. c_s. Also, if $P(k) \propto k^{-n}$, then

$$v(l) \propto \sigma_v(l) \propto \Delta v(l) \propto l^q \tag{97}$$

with $q = (n-3)/2$.
If the system is considered spatially symmetric with each dimension $\approx l$, then the one-dimensional velocity dispersion along a given line-of-sight can be related to the 3D velocity dispersion by $\sigma = \sigma_v(l)/\sqrt{3}$

2.9.3 Brief Review of Some Models

If the turbulent system is closed with appropriate periodic and boundary conditions, a number of invariants are considered in the ideal limit $\mu = \eta = 0$ ([51]). For incompressible, three dimensional MHD, these irregular ideal invariants are given as follow with their decay rates at finite viscosity and magnetic diffusivity. (explanation follows from [47])
Total Energy

$$E = E^K + E^M = \frac{1}{2}\int_V dV\,(v^2 + b^2)\ ,\ \dot{E} = -\int_V dV\,(\mu\omega^2 + \eta j^2) \tag{98}$$

Magnetic Helicity

$$H^M = \frac{1}{2}\int_V dV(a)\ ,\ \dot{H}^M = -\eta\int_V dV\, j\cdot B \tag{99}$$

Cross helicity

$$H^C = \frac{1}{2}\int_V dV(v\cdot b)\ ,\ \dot{H}^C = \frac{\mu+\eta}{2}\int_V dV\,\omega\cdot j \tag{100}$$

These three ideal variants are quite important in characterizing the macroscopic properties of MHD turbulence. Due to statistical homogeneity alongwith quasi-ergodocity hypothesis, we can replace ensemble averages by spatial time averages by neglecting the influence of distant boundaries. Periodic conditions are then applied at the surface outside of volume V which contains the turbulent flow.

One of the most famous model of turbulence for subsonic, hydrodynamic turbulence is the K41 theory given in [52]a, [53]b. However, it doesn't include magnetic field. Real interstellar clouds aren't actually subsonic and hydrodynamic ([49]).

Using the K41 picture, we can differentiate three spatial scale ranges:

- the energy containing scales which drive flow
- dissipation range at smallest scales, where dissipative effects dominate
- the inertial range where non-linear interaction which influence the driving, dissipation and govern the dynamics are negligible

(the explanation follows from [47] As is experimentally observed that structure functios of order p , $S_p^v(l) = \langle \delta v_l^p \rangle$ follows power-laws in l with constant $p-$ dependent exponents ζ_p. As K41 theory builds up, it predicts values for scaling these exponents in the limiting case of infinite R_e. The treatment of K41 in the sense of aymptotic statistical variance properties of real-turbulence is given in detail in [45]. Also, an important realization of Kolmogorov was that in the spatial hierarchy of eddies, the larger ones transfer a fraction of their energy(i.e. resulting energy flux) towards smaller counterparts ([54]), the size of interacting eddies differing only slightly i.e. the transfer proceeds in small local steps in spatial Fourier space. These *cascades* are usually considered to be cause by non-linearities in Navier-Stokes and MHD equations. The energy flux is estimated by order of magnitude as ${v_l}^2/\tau_l$ with the non-linear eddy turnover time $\tau_l = l/v_l$

In a fully-developed turbulence, where we include all the assumptions explained above, the non-energy flux in the inertial-range equals the energy dissipation ϱ which gives by order of magnitude

$$\varrho \sim \frac{{v_l}^2}{\tau_l} = \frac{{v_l}^3}{l} \implies v_l \sim (\varrho l)^{1/3} \implies S_3^v(l) = -\frac{4}{5}\varrho l \tag{101}$$

The Fourier transform of S_2^v scales as the one-dimensional energy spectrum defined as $E_1(k_1) = (1/2)\int dk_2 \int dk_3\, \boldsymbol{v(k)} \cdot \boldsymbol{v^*(k)}$ with $k_i = (2\pi/l_i)$ Here, since turbulent is taken to be isotropic, so the angle-integrated energy spectrum

$$E(k) = \int_0^{4\pi} d\Omega\, E(k)|_{|k|=k} \tag{102}$$

defining $E(\boldsymbol{k}) = (1/2)|\boldsymbol{v(k)}|^2$, The real space exponent ζ_2 of $S_2^v(\boldsymbol{l})$ corresponds to an inertial range Fourier-space scaling $\sim k^{-1+\zeta_2}$ which yields the experimentally well supported **Kolmogorov spectrum**

$$E(k) = C_k\, \varrho^{2/3}\, k^{-5/3} \tag{103}$$

with the Kolmogorov constant $C_k \approx 1.6$ The **Kolmogorov disspation length** l_{K41} gives an order of magnitude estimate of the spatial scales where energy dissipation $\sim v_l^2 \mu / l^2$ begins to dominate the non-linear energy dynamics $\sim v_l^2/\tau_l$ that marks the beginning of dissipation range. With the approximations above,

$$\frac{\mu}{l^2} \sim {\tau_l}^{-1} = \frac{v_l}{l} \sim \frac{(\varrho l)^{1/3}}{l} \implies \boldsymbol{l_{\text{K41}}} = \left(\frac{\boldsymbol{\mu^3}}{\boldsymbol{\varrho}}\right)^{1/4} \tag{104}$$

(the explanation follows from [4]) Important point to note that, because velocities $v(l) \sim {}_v(l) \sim \Delta v()$ in molecular clouds are in general not small compared to c_s, for sufficiently large l, so one cannot expect Kolmogorov theory to apply. Even, some portion of energy at a given scale is directly dissipated via shocks rather than by *Richardson cascading*, there are a network of intersecting shocks in the limit of zero pressure, also known as *Burger's turbulence* ([55]). Since the power spectrum corresponding to a velocity discontinuity in one-dimension has $P(k) \propto k^2$, an isotropic system of shocks in three dimensions would also yield power-law scalings for the velocity correlations, with $n = 4$ and $q = 1/2$. Note that these correlations can be expressed in a power-law form even if there's not any case of conservative inertial cascade

Turbulence in a magnetized system is inherently different from unmagnetized case because of the additional wave families, non-linear couplings and additional diffusive processes (including resistive and ion-neutral drift terms) involved. In the case, magnetic field B is strong, the Alfvén velocity v_A satisfies $v_A \gg v(l)$, here a directionality is introduced such that correlations of the flow variables depend differently on $r_\parallel$, $r_\perp$, $k_\parallel$ and $k_\perp$, that are the displacement and wavevector components parallel and perpendicular to $\hat{B}$

The IK i.e. Iroshnikov-Kraichnan phenomenology for MHD turbulence is just a modification of K41 approach while introducing a different model for non-linear flux. (see [56], [57] for more detail on IK picture).
The K41 and IK models are spatially isotropic in a way that turbulent structures are characterized by a single length scale l. However, in the presence of the magnetic field B, the characteristic interaction time of Alfvén wave like distortions of extent λ along the field lines $tau_l \sim \lambda/b_0$ is way shorter than non-linear turnover time $\tau_l \sim l/z_l$ of their components of extent l and amplitude z_l

$\perp B$. Furthermore, non-linear energy flux shows a clear anisotropy.([58], [59]) (explanation follows from [47]).
Against this background, for *incompressible* MHD, Goldreich and Sridhar developed a semi-phenomenological GS95 model ([60], [61; 62]), where they introduced the idea of a critically-balanced anisotropic cascade, in which the non-linear mixing time $\perp B$ and propagation time $\parallel B$ remain comparable for wavepackets at all scales, so $v_A k_\parallel \sim v(k_\perp, k_\parallel)k_\perp$. Interactions between oppositely-directed Alfvén wavepackets travelling along B cannot change their parallel wavenumbers $k_\parallel = l \cdot \hat{B}$, so that energy transfers produced by these collisions involve primarily $k_\perp$ i.e. cascade though spatial scales $l_\perp = 2\pi/k_\perp$ with $v(l_\perp)^3/l_\perp \sim$ constant. Fusing critical balance with a perpendicular cascade yields anisoptropic power spectra (larger in $k_\perp$ direction); at a given level of power, the theory predicts $k_\parallel \propto {k_\perp}^{2/3}$ and magnetic fields and velocities have the same power spectra.

But if see the case of strong compressibility ($c_s \ll v$ and moderate or strong magnetic fields ($c_s \ll v_A \lesssim v$), which usually applies within molecular clouds, there is as of yet, no simple conceptual theory, to characterize the energy transfer between scales and to describe the spatial correlations in the velocity and magnetic fields. On universal scale, the flow can be dominated by large-scale (magnetized) shocks which directly transfer energy from macroscopic to microscopic degrees of freedom. Even if velocity differences are insufficient to induce sufficient shocks, for trans-sonic motions compressibility implies strong coupling among all MHD wave families. However, within a sufficiently small sub-volume of a cloud (*away from shock interfaces*), velocity differences may be sufficienty subsonic that the incompressible MHD limit and the Alfvénic cascade, such as in GS model, hold approximately in a local region.

Intermittency effects (i.e. one of the crucial properties of turbulence is unfortunately not considered in classical models of turbulence. The K41 and IK models, which implicitly assume spatial uniformity of energy dissipation ϱ give the scaling exponents ζ_p of structure functions of order p as $\zeta_p^{\mathsf{K41}} = p/3$ and $\zeta_p^{\mathsf{IK}} = p/4$. There is however, seen to deviations of high-order structure function exponents from the value $p/3$ and in non-Gaussian tales of velocity increment probability-distribution functions (PDFs) (Sreenivasan and Antonia [63], Lis et al. [64]) in the turbulent solar wind (Burlaga [65]) as well as direct numerical simulations(DNS) of MHD turbulence (Politano, H. et al. [66], Biskamp and Müller [67]; Biskamp and Müller [68]). The *anomalous scaling* is attributed to departure from self-similarity of turbulent fields in the inertial range, the effect of which is linked to the spatial distribution of the turbulent structures responsible for energy dissipation by Kolmogorov's refined similarity hypothesis(Kolmogorov [69])that introduces the local energy dissipation in a sphere of radius l, ϱ_l. Instead of spatial homoegeneous distribution of energy dissipation, the turbulent system is interspersed with small regions of intense dissipation, resulting in a pronounced spatial intermittency.

Some models which account for intermittency in prediciting correlation functions for incompressible, unmagnetized turbulence are (She and Leveque [70],Dubrulle [71]. Boldyrev [72] proposed for a model for the compressible MHD case, but in that the direct dissipation of large-scales modes in shocks was omitted. Research on formal turbulence theory is still quite an active field (see Elmegreen and Scalo [43] for a review of the recent theoretical literature in this area) yet a comprehensive framework is still to be seen. For a review of recent numerical simulations validating some of the above models such as the SL picture, and other developments in the theory of turbulence see McKee and Ostriker [4]. For review on extensions of incompressible theory, see Falgarone and Passot [47]

2.9.4 Further on Interstellar Turbulence

All turbulent systems seem to share one common thing i.e. a large Reynold's number. The properties of the flows on all scales depend on R_e and R_m. Flows with $R_e < 100$ are laminar, chaotic structures develop gradually as R_e increases, and those with $R_e \sim 10^3$ are considerably less chaotic than those with $R_e \sim 10^7$. Observations of star forming clouds and accretion disks are very chaoticwith $R_e > 10^8$ and $R_m > 10^{16}$. ([47])
As mentioned in the previous section, turbulence plays a critical role in molecular cloud support and star formation and the issue of the time scale of turbulent decay is quite an important subject of discussion. The decay of MHD turbulence poses problems in understanding things such as turbulent motions seen within molecular clouds without star formation([73]) and rates of star formation([74]). Earlier studies have attributed the rapid decay of turbulence to compressibility effects ([75]). GS95 predicts and numerical simulations e.g. CLV02a, confirm that MHD turbulence decays rapidly even in the incompressible limit. The effect of imbalance (i.e. flux of wave packets travelling in one direction is significantly larger than those travelling in opposite direction) ([76], [77], [78], [79], [80]) on the turbulence decay time scale. In the ISM, many energy sources are localized, both in space and time. For e.g., in terms of energy injection, stellar outflows are essentially point energy sources. With these localized energy sources, it is natural that interstellar turbulence be typically imbalanced. (follows from [47], see more for detail on interstellar turbulence)

2.9.5 Observation of Magnetic Fields

Observation of magnetic fields is critical to elevating our understanding about various processes in the galactic formation in which magnetic fields have been shown to play a part either through simulations, theoretical models or through observations.Here, we would be giving an extremely brief review, taking points from some sources which give exhaustive reviews in this field ([47], [4]). As we know, the stars are weakly magnetized, while the interstellar medium is strongly magnetized. The strength and morphology of uniform (B_u) and random (B_r) components of magnetic fields in Galactic Scales has been area of much intensive research for a long time, since the discovery of the interstellar polarization of starlight.

The role of magnetic fields in star formation process has been the subject of many theoretical and observational investigations([81]). Recent reviews include those of [74], [2], [82]). An important question is whether or not magnetic energy density is comparable to other energy densities, such as gravitational, thermal and turbulent. If that's true, then magnetic fields must play a significant role in cloud evolution and star formation while if that's false, then their role can be either secondary or even unimportant. There are two ways which this question can be structured, one is by asking "What is the magnetic field morphology?" and the other is "What is magnetic field strength"? (see Magnetic field observations in [47] for more detail)

In order to verify the theoretical models, and observe the presence of presence of magnetic fields and their strength and influence, observational techniques are used.([4]) Two primary observational methods to measure the magnetic field strengths in dense ISM are Zeeman effect (measures the line of sight component, B_{los} and the Chandrashekhar-Fermi (CF) method ([23]) that measures the field component in the plane of sky, B_{pos}, by comparing the fluctuation in the direction of B_{pos} with those in the velocity field(see reviews by [83], [84]). The morphology of the field which is needed for CF

method is measured from dust polarization and from linear polarization of spectral lines.([85]) In the diffuse ISM, magnetic fields are also obtained by Faraday rotation and synchroton observations, with results consistent with Zeeman observations (see [86] for more detail on observational techniques, for development in brief, see ([4])

2.9.6 Turbulence Driving Parameter

Turbulence driving parameter is an important dimensionless constant, and the recent years have seen a lot of development on it. Here we would be taking pointers from some of the excellent reviews out there on the topic such as ([87], [88] etc.)

Turbulence regulates the star formation in molecular clouds and plays a dual role in the process by providing a form of support against self-gravitational collapse due to random velocity fluctuations, and on the other hand forming shocks resulting in overdensities that eventually undergo gravitational collapse.(Mac Low and Klessen [3])
As discussed before briefly in the Introduction to this Chapter,on the variety of turbulent driving mechanisms observed, all of these mechanisms act on different spatial scales but the basic difference lies in the type of turbulent modes they drive: compressive (curl-free) or solenoidal (divergence free) modes. Whether turbulence is driven compressively or solenoidally generates quite considerable implications on the evolution of gas in molecular clouds.

For e.g. in Federrath and Klessen [89], star formation rate(*will be discussed in detail later*) in simulation was found to be 10 times larger in the case of compressive driving than solenoidal driving of turbulence. In the simulations of Renaud et al. [90], galaxy mergers increased the power in compressive fluid motions, leading to enhanced star formation. As compressive driving is associated with gravitational collapse of gas and supernovae, it may also be associated with recent or a future occuring star formation. On the other hand, solenoidal driving, tends to be associated with quiescent gas Federrath et al. [91]. So, the relative strengths of compressive and solenoidal driving determines the structure and star formation in molecular clouds.

Federrath et al. [91] introduced the turbulent driving parameter b, to descirbe the relative strengths of compressive and solenoidal modes. Through this parameter, the ratio of power in compressive forcing modes F_{comp} relative to the total forcing power $F_{\mathsf{total}} = F_{textcomp} + F_{\mathsf{sol}}$, where F_{sol} is the power in solenoidal forcing modes.

$$\frac{F_{\mathsf{comp}}}{F_{\mathsf{total}}} = \frac{(1-b^2)}{(1-2b+Db^2)} \tag{105}$$

The above equation defines b. Here, D is the number of spatial dimensions. The parameter b is defined such that $b \in [0,1]$ where $b = 0$ for purely compressive driving and $b = 1$ for purely solenoidal driving. 'Natural mixing' of turbulence corresponds to one-third of the injected energy going into the compressive modes, as these modes are longitudinal and occupy one of the spatial dimensions.

Based on more observations and simulations(such as [92]), the value of b was improved, it varies between $1/3$ and 1, where these two extreme cases refer to purely solenoidal and purely compressive

driving, respectively, with a natural mixture of solenoidal and compressive modes at $b \sim 0.4$ (see figure 8 in [91] too, [88], [87]).
The value of b is important, as the flow dynamics, density structure and the subsequent star formation rate depends on it ([93; 91], [94], [95], [44], [96], [97]; with compressive driving resulting in broader density probability distribution functions(PDFs) and star formation rates approximately an order of magnitude larger than for solenoidal driving.([89], [98], [99]). The values of b has been systematically studied too for different driving sources of turbulence in numerical simulations and observations also find a significant variation in b across different clouds in the Milky way. (see [87]) and the references contained there in for greater detail).

3 Development of Mathematical Model

Consider a uniform, isothermal, turbulent, magnetized SFC-GMC at rest with density ρ, pressure p and temperature T, which are constant everywhere. Note that this state is not a well-defined equilibrium. The assumption of isothermal gas is very crude, but may still provide an adequate physical approximation to the real thermodynamics in dense molecular gas([100], [101], [91]). Here, the gas cloud is described by the Navier-Stokes equations.

3.1 Expressions Relating Star formation Rate (SFR)

Star formation rate(SFR) is the total mass of stars formed per year but mathematically defined as integral of log-normal density Probability Density Function (PDF) by weighing the density fraction ρ/ρ_0 to get mass fraction and then subsequently weighted by free-fall time factor to get the dimensionless rate. Star Formation Rate submits to Kennicut-Schmidt law, which is given as (derived from first principles in [102]).

$$\sum_{*}^{\cdot} \propto \sum_{g}^{1.4} \tag{106}$$

where $\sum_*$ is the SFR per unit area, $\sum_g$ is the surface density of gas. The coefficients and exponents in Equation (106) were characterised by Kennicut from large sample of galaxy.

To derive SFR we initially need to compute Star Formation Rate at free-fall time t_{ff}. From the observations and simulations of turbulence it has been noticed that turbulence in Interstellar medium (ISM) shows that turbulent velocity dispersion σ_v computed over a large volume say characteristic length l increases with length as [103]

$$\sigma_v \propto l^p \tag{107}$$

Where p is taken as $1/2$. This structure is taken as universal property of supersonic turbulence and it holds for wide range of length as in kpc in the matter of Giant molecular clouds [104] [105] (GMCs).
Let $\sigma_v\, x$ be the one-dimensional velocity dispersion computed over a sphere of diameter say l centered at position s in turbulent medium,

$$\sigma_v = \langle\, \sigma_v\, s \,\rangle_V \tag{108}$$

where V is the volume of verge of $\sigma_v\, s$
Now, we define l_s, known as sonic length, scale at which turbulence advances from supersonic to subsonic and this assumes significant part in determining whether SFR_{ff} will be high or low.[106] Here, we take $\sigma_v = c_s$, where c_s is the isothermal speed of sound in the particular region of molecular cloud. Henceforth, the velocity dispersion correlation becomes,

$$\sigma_v = c_s \left(\frac{l}{l_s}\right)^p \tag{109}$$

here SFR_{ff} is dimensionless number and sonic length is just length [3], subsequently we take another relevant scale which is known as Jeans scale. The Jeans Length is characterised as,

$$\lambda_j = \sqrt{\frac{\pi {c_s}^2}{G\rho}} \tag{110}$$

where ρ is the density of gas. As we have considered turbulent medium, where ρ changes with position. In order to observe the impact of changing density, assume a small sphere of gas embedded inside the molecular cloud,thermal pressure at the surface of this sphere will be $\rho\, {c_s}^2$. [107] The largest mass such an object can have and furthermore stay stable against the gravitational collapse is known as Bonnor-Elbert mass ([108]), which is given as,

$$M_{BE} = \frac{1.18\, {c_s}^3}{\sqrt{G^3\rho}} = \left(\frac{1.18}{\pi^{3/2}}\right) \rho {\lambda_j}^3 \tag{111}$$

let us take the radius of such sphere say R_{BE} can be taken as $0.37\lambda_j$ The gravitational potential energy of sphere can be defined as,

$$W = -\frac{3\, a\, G M_B E^2}{5\, R_{BE}} = -1.06 \left(\frac{{c_s}^5}{G^{3/2}\, \rho^{1/2}}\right) \tag{112}$$

here a is geometric factor which is set by considering mass distribution of the sphere taken into account and for numerical methods it's value is taken as $a = 1.2208.$ which is also the value for maximum mass stable Bonnor-Elbert sphere.([108], [4]) Thermal energy of the gas is given by,

$$T_{th} = \frac{3}{2}\, {c_s}^2\, M_{BE} \; = 1.14W \tag{113}$$

using the equation (109) we find the average turbulent kinetic energy of sphere,

$$K_{tur} = \frac{3}{2} M_{BE}\, \sigma^2\, R_{BE} = 0.89 \left(\frac{\lambda_j}{\lambda_s}\right) W \tag{114}$$

Thus, Bonner-Elbert mass sphere will have equal kinetic, thermal and potential energy if $\lambda_j \approx \lambda_s$. And if $\lambda_j \leq \lambda_s$ then gravity will be balanced by thermal plus turbulent pressure and sphere will be barely stable against the collapse, but if $\lambda_j \geq \lambda_s$ then kinetic energy surpasses the potential and thermal energy and sphere is stable against collapse. ([109], [110], [111])
Since λ_s here is local density, the condition $\lambda_j \leq \lambda_s$ for collapse translates it into minimum required density essential for collapse. We will use this to compute SFR by integrating log-normal density PDF by taking ρ/ρ_0 to get mass fraction of gas, according to ([112], [113]) PDF is given as,

$$dp(s) = \frac{1}{\sqrt{2\pi\sigma_s^2}} \exp\left(-\frac{\ln s - \ln s_0}{\sigma_s^2}\right) \frac{d(s)}{s} \tag{115}$$

where in equation (115), s is logarithmic density and it is related with density as $s = \ln(\rho/\rho_0)$, and s_0 is logarithmic mean density which is related with density dispersion as,

$$\ln s_0 = -\frac{1}{2}{\sigma_s}^2 \tag{116}$$

Due to normalization and mass-conservation constraints.[114] The reason we have utilized s rather than ρ in the context of density PDF is on the grounds that s is dimensionless and the PDF of s is

Gaussian unlike the PDF of ρ .[115] Since, $s \propto \ln \rho$ as defined above the multiplicative interaction in ρ becomes additive process in s, consequently following the central limit theorem, a large sum of random variables produces a Gaussian distribution, and thus only p_s is Gaussian and $p\,\rho$ is not ([27], [116]). While the standard deviation is given by,

$$\sigma_s = \ln \sqrt{1 + \frac{3\mathcal{M}^2}{4}} \tag{117}$$

where $\mathcal{M}$ is the one-dimensional Mach number in turbulent medium. In our case we have taken few parameters to analyse the star formation rate and those are 1) turbulent forcing parameter (b), 2)magnetic field (B). The reason why we have considered above mentioned factors, is that even though we initially thought that magnetic field would provide stability against gravitational collapse only after the diffusion of neutral species via charged particles before star formation ([117], [104], [118]). However, during ambipolar-diffusion, magnetic flux is left behind in the envelope, while the mass goes on increasing in the core.[119].Also, we have observed supersonic random motion, which might regulate the star formation rate. [120] where turbulent energy stabilizes the clouds on large scales while supersonic turbulence also induces local compression. [121] Therefore, we determined that both these factors are essential in accurately determining star formation rates. ([122], [104], [123])
To define standard deviation in terms of b, β and $\mathcal{M}$ we will modify the equation (117) which is given by,

$${\sigma_s}^2 = \ln\left(1 + b^2\mathcal{M}^2\frac{\beta}{\beta+1}\right) \tag{118}$$

where β is ratio of thermal to magnetic pressure which is given as,

$$\beta = \frac{P_{th}}{P_{mag}} = \frac{8\pi\,\rho\,{c_s}^2}{B^2} \tag{119}$$

The standard deviation in the equation (118) is a proportion of how much the density varies in a turbulent medium, and thus relies upon (i) the amount of compression injected by b i.e. turbulence driving parameter, (ii) Sonic Mach no. $\mathcal{M}$, and (iii) the degree of magnetization. [124] To define critical density s_crit we have to take Jeans Length into account, which are λ_J and λ_{j0} called Jeans Length at density and Jeans Length at mean density respectively. [125] Hence critical density is defined as,

$$s \geq s_{crit} = \left(\phi_x\,\frac{\lambda_{j0}}{\lambda_j}\right)^2 \tag{120}$$

where ϕ_x is numerical factor, whose value is $\phi_x = 1.12$ Hence the fraction of mass for collapsing sphere is just fraction of mass at density of s_{crit} or greater which is given as,

$$f = \int_{s_{crit}}^{\infty} s\left(\frac{dp}{ds}\right)\,ds \tag{121}$$

To convert this mass fraction into SFR we will take two factors into consideration, one is outflow which is defined as ϵ_{ff}, whose theoretical limits are $0.3 - 0.7$ [126] second, we have taken it's best fit value which is 0.5 second. With these two factor defined the SFR per free-fall time is,

$$\begin{aligned} \text{SFR}_{\text{ff}} &= \frac{\epsilon_{\text{ff}}}{\phi_t}\int_{s_{crit}}^{\infty} s\,p(s)\,ds \\ &= \frac{\epsilon_{\text{ff}}}{\phi_t}\left(\frac{t_{\text{ff}}(\rho_0)}{t_{\text{ff}}(\rho)}\right)\frac{\rho}{\rho_0}\,p(s)\,ds \end{aligned} \tag{122}$$

Note that $t_{\mathrm{ff}}(\rho_0)/t_{\mathrm{ff}}(\rho)$ appears inside the integral because gas with different density have different free-fall time. Hence the SFR of cloud of mass M_c is,

$$\mathrm{SFR} = \mathrm{SFR}_{\mathrm{ff}} \left(\frac{M_C}{t_{\mathrm{ff}}}\right) \tag{123}$$

By inserting equation (115) and (122) into equation (123) we get expanded version of SFR which we have used for numerical and computational evaluation,

$$\mathrm{SFR} = \frac{\epsilon_{\mathrm{ff}}}{\phi_t}\int_{s_{crit}}^{\infty} \frac{t(\rho_0)}{t_{\mathrm{ff}}(\rho)}\,\frac{\rho}{\rho_0}\,\frac{1}{\sqrt{2\pi\ln\left(1+b^2\mathcal{M}^2\frac{\rho {c_s}^2}{\rho {c_s}^2+B^2/(8\pi)}\right)}}\,\exp\left(\frac{-(S-S_0)^2}{2\ln\left(1+b^2\mathcal{M}^2\frac{\rho {c_s}^2}{\rho {c_s}^2+B^2/(8\pi)}\right)}\right) dS \tag{124}$$

3.2 Role of Magneto-hydrodynamics (MHD) in Giant Molecular Cloud (GMC)

In our model we have considered ideal MHD equation including self-gravity with poly-tropic equation of state, as the gas in the sphere is considered to be isothermal with the speed of sound c_s. The equations are defined as,

$$\frac{\partial \rho}{\partial t} + \boldsymbol{\nabla}\cdot(\rho v) = 0, \tag{125}$$

$$\rho(\frac{\partial}{\partial t} + v\boldsymbol{\nabla}\cdot)v = \frac{(B\boldsymbol{\nabla}\cdot)B}{(4\pi)} - \boldsymbol{\nabla}\times P_* + \rho(g+F_*), \tag{126}$$

$$\frac{\partial E}{\partial t} + \boldsymbol{\nabla}\cdot(E+P_*)v - \frac{(B\boldsymbol{\nabla}\cdot v)B}{(4\pi)} = \rho v\boldsymbol{\nabla}\cdot(g+F_*), \tag{127}$$

$$\frac{\partial B}{\partial t} = \boldsymbol{\nabla}\times(v\boldsymbol{\nabla}\times B), \tag{128}$$

$$\boldsymbol{\nabla}\cdot B = 0 \tag{129}$$

where ρ , P_*, g , E , v are density, pressure (thermal + magnetic), gravitational acceleration of gas, energy density, and velocity respectively. The polytropic equation of state is characterised by,

$$P_{th} = {c_s}^2\,\rho^l \tag{130}$$

where, $l = 1$ for isothermal gas
Above equations shows that the MHD keeps $\boldsymbol{\nabla}\cdot B$ at negligible level, allow us to simulate high mach number turbulence without generating non-physical state. ([127]). This is particularly essential for this study because in our numerical model we consider compressive and solenoidal forcing, which produces density contrasts by several orders of magnitude, due to multiple interactions of shocks and strong rarefaction waves, even before gravitational collapse sets in.([128], [100])

4 Computational Analysis of Model

The generalized mathematical model taken gives us a relation between SFR, magnetic field B, turbulence driving parameter b and some previously mentioned non-dimensional parameters such as β, $\mathcal{M}$ and so on. As covered in the Background Literature Review and mathematical model, SFR has been shown to depend upon four parameters :

- Virial Parameter α_{vir}
- Plasma Beta Parameter β
- Sonic Mach Number $\mathcal{M}$
- Turbulence Driving Parameter b
- Mass-flux ratio μ_Φ

The final equation would be using to do our simulations would be Equation (124), that is

$$\text{SFR} = \frac{\epsilon_{\text{ff}}}{\phi_t}\int_{s_{crit}}^{\infty}\frac{t(\rho_0)}{t_{\text{ff}}(\rho)}\frac{\rho}{\rho_0}\frac{1}{\sqrt{2\pi\ln\left(1+b^2\mathcal{M}^2\frac{8\pi\rho {c_s}^2}{8\pi\rho {c_s}^2+B^2}\right)}}\exp\left(\frac{-(S-S_0)^2}{2\ln\left(1+b^2\mathcal{M}^2\frac{8\pi\rho {c_s}^2}{8\pi\rho {c_s}^2+B^2}\right)}\right)dS \tag{131}$$

In this model we have considered two parameters b and B, to study their influence on SFRs.
In our simulations, we take $b \in [1/3, 1]$ (based on discussion in 2.9.6 Turbulence Driving Parameter) and $B \in [1, 10]; B \in \mathbb{N}$ in units of μG. Here, we would be varying both b and B in the given ranges selectively to see their effect on SFRs of some clouds.
The dataset we would be using is from [129], and the table we have extracted from there is as given here as Table 1, consisting of 10 randomly chosen SFC-GMC complexes from Milky Way and some of their star formation properties(v , σ_v , Σ_g , α_{vir} , t_{ff} , M_g) which we would be taking into consideration.
For simplicity of identification, we have assigned each of the SFC-GMC chosen, a Gas Cloud No. from 1 to 10 as given in the Table 1.

Here, we would be taking $\mathcal{M} \sim 10$, which may look like strong assumption but it gives a good indication of the role of magnetic fields for typical molecular cloud properties. (e.g. [130], [131], [89])

Equation (131) was translated into a Python program. Fundamental modules like 'numpy' and 'math' were used to construct the code. Numpy arrays and NumPy ufunc were used to get required results simultaneously for 10 clouds. The data was collected for observing variation of b and B w.r.t SFR for these randomly chosen SFC-GMC complexes and later plotted the variations using MATLAB.

In the Fig. 1 , we fixed $b \sim 0.4$ i.e. natural mixing of solenoidal and compressive driving modes and plotted the variation of SFRs w.r.t B from $[1, 10]\mu G$ for each of 10 SFC-GMCs
In Fig 2 (a,b,c,d,e,f,g,h,i,j), in each of the graphs, we fix B at $[1, 10]\mu G$ and get the plots of SFR vs b where $b \in [1/3, 1]$ and each figure is such a plot for each SFC-GMC.

Table 1: **Star-Formation Properties of 10 SFC-GMC Complexes from Milky Way (Sorted by Luminosities)**

SFC No.	Cloud no.	v (km s^{-1})	σ_v (km s^{-1})	α_{vir}	$\tau_{\rm ff}$	R (pc)	$\epsilon_{\rm ff,\ br}$	$M_g\,(M_\odot)$	$\Sigma_g\,(M_\odot {\rm pc}^{-2})$
227	1	-75.34	10.80	9.58e+00	9.32	66.84	9.14e-01	9.47e+05	6.31e+01
228	2	-55	7.65	9.58e-01	7.41	119.13	5.77e-02	8.49e+06	1.61e+02
68	3	98.41	5.34	6.90e-01	4.66	61.64	5.69e-02	2.97e+06	2.23e+02
111	4	-3.21	3.48	2.83e-01	5.26	70.60	4.79e-02	3.51e+06	2.18e+02
274	5	-1.41	9.37	2.82e+00	5.61	64.29	6.86e-02	2.33e+06	1.51e+02
2	6	15.44	3.30	6.98e-01	5.22	42.39	1.71e-01	7.69e+05	1.13e+02
249	7	-95.96	6.88	3.54e+00	7.97	59.93	1.99e-01	9.33e+05	7.36e+01
110	8	-1.04	3.75	3.49e-01	5.62	73.23	3.90e-02	3.43e+06	1.88e+02
72	9	102.25	5.59	1.55e+00	5.73	52.90	1.03e-01	1.24e+06	8.71e+01
191	10	-50.97	5.53	7.67e-01	4.45	57.79	3.80e-02	2.69e+06	2.34e+02

(table extracted from Table 2, 3 of [129])

**Note that the order of SFC no's appear shuffled because here they have adopted mass-weighted distances of matched GMCs for each SFC here. The physical radius R is defined as $d\tan(R_{\rm ang})$. The gas surface density $\Sigma_g = M_g/(d\tan(\pi R_{\rm max} R_{\rm min})^2$ while the virial parameter $\alpha_{vir} = 5{\sigma_v}^2 R/GM_g$ and $\epsilon_{\rm ff,\ br}$ is as defined in the paper [129]

5 Star Formation Rate(SFR) vs Magnetic Field (B)

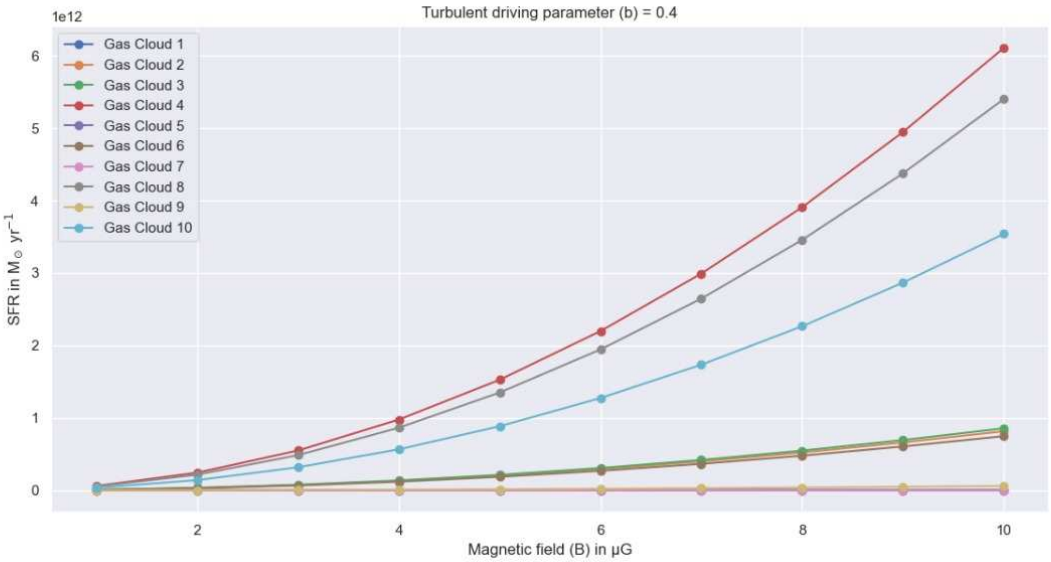

Figure 5.1: SFR vs B

In Cloud 7, the general trend seen is decrease in SFR as B increases, while all the other clouds show increase in SFR as B increases.

6 Star Formation Rate(SFR) vs Turbulence Driving Parameter (b)

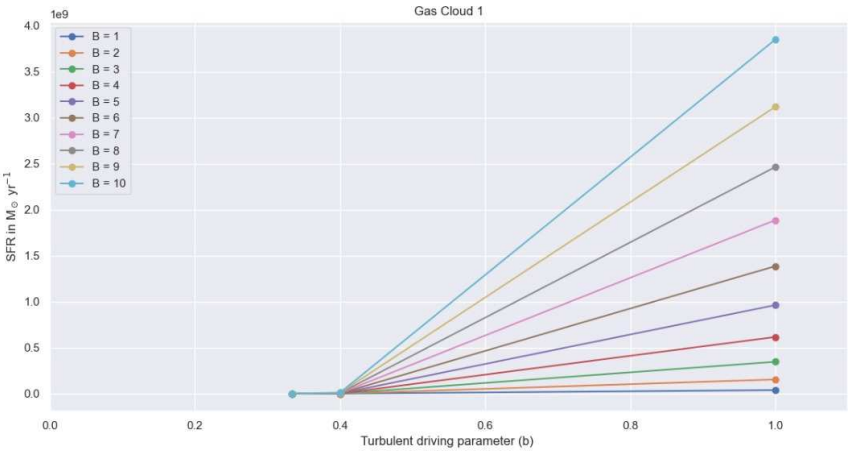

Figure 6.1: SFR vs b for Gas Cloud 1

A general increase in SFRs as b increases is seen when Magnetic Field i.e B is fixed.

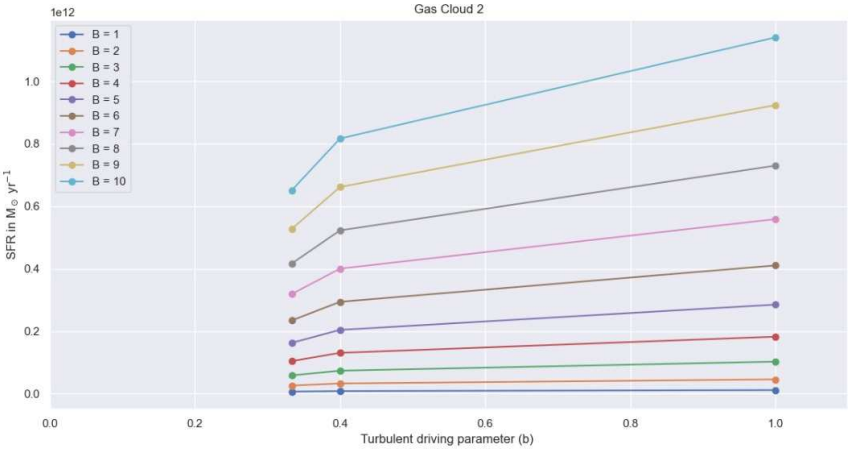

Figure 6.2: SFR vs b for Gas Cloud 2

A general increase in SFRs as b increases is seen when Magnetic Field i.e B is fixed.

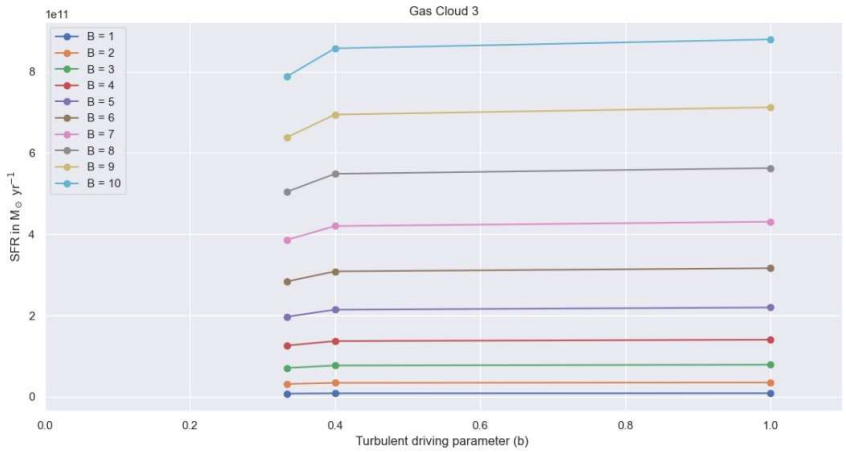

Figure 6.3: SFR vs b for Gas Cloud 3

A general increase in SFRs as b increases is seen when Magnetic Field i.e B is fixed.

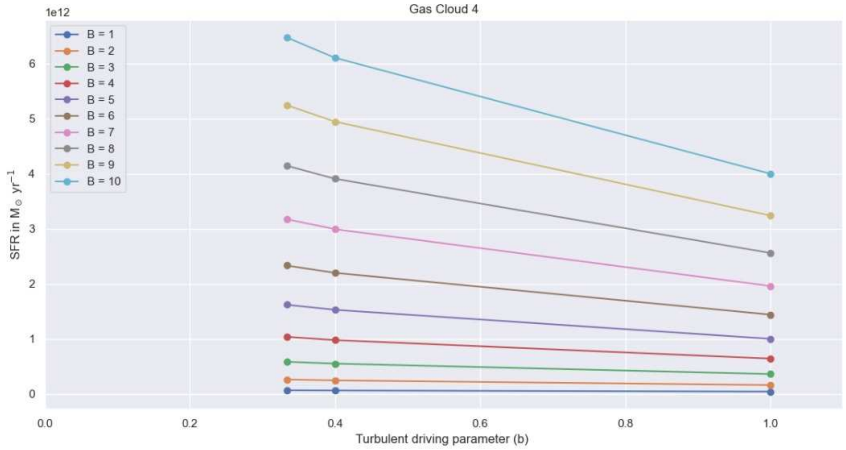

Figure 6.4: SFR vs b for Gas Cloud 4

A general decrease in SFRs as b increasing is observed with a converging trend while Magnetic Field i.e B is fixed .

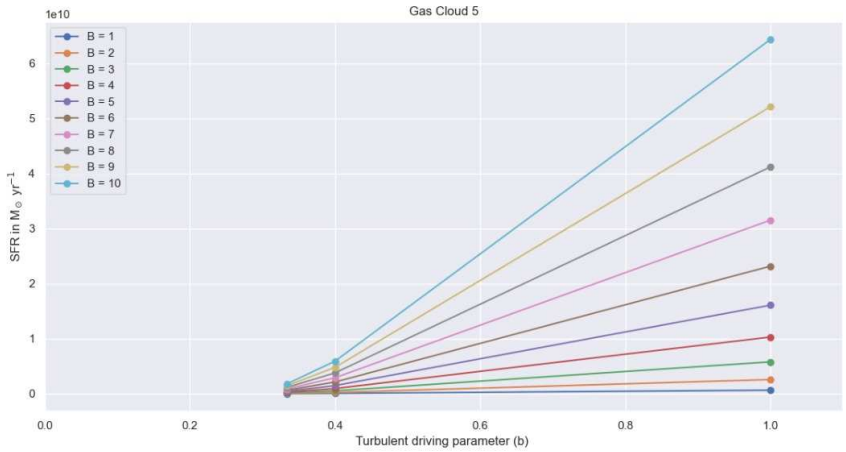

Figure 6.5: SFR vs b for Gas Cloud 5

A general increase in SFRs as b increases is seen when Magnetic Field i.e B is fixed.

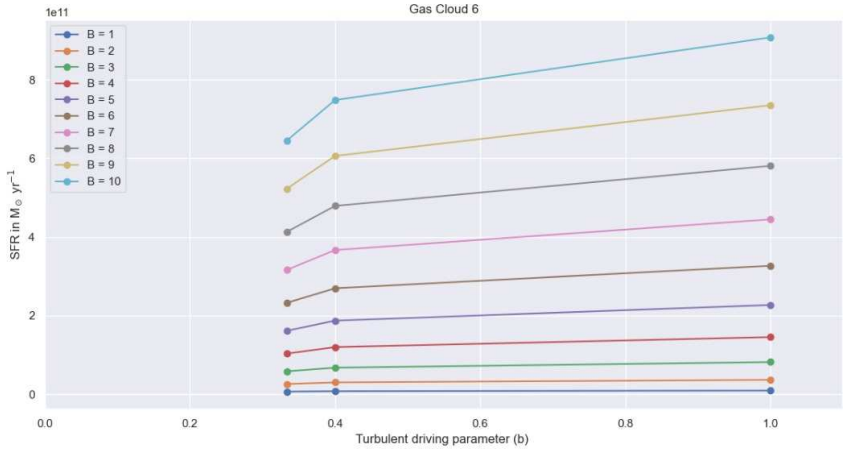

Figure 6.6: SFR vs b for Gas Cloud 6

A general increase in SFRs as b increases is seen when Magnetic Field i.e B is fixed.

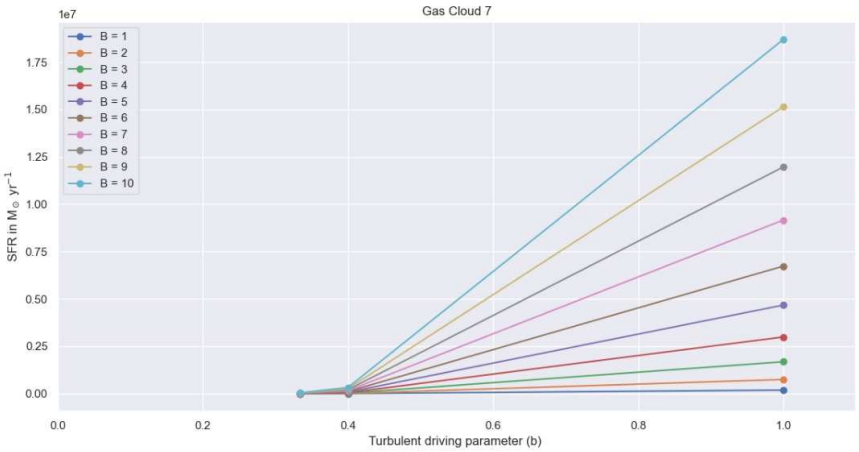

Figure 6.7: SFR vs b for Gas Cloud 7

A general increase in SFRs as b increases is seen when Magnetic Field i.e B is fixed.

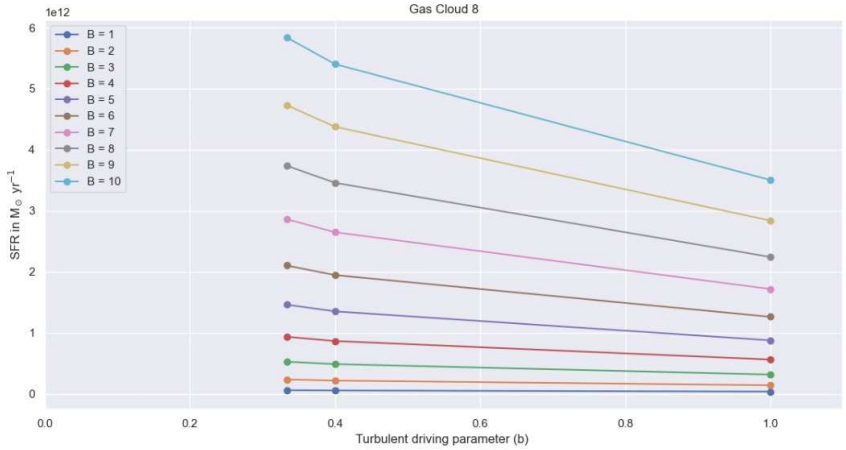

Figure 6.8: SFR vs b for Gas Cloud 8

A general decrease in SFRs as b increasing is observed with a converging trend while Magnetic Field i.e B is fixed .

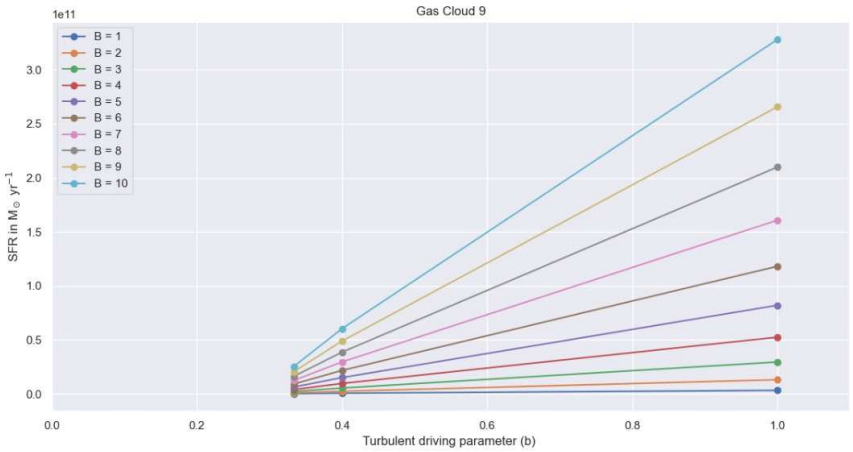

Figure 6.9: SFR vs b for Gas Cloud 9

A general increase in SFRs as b increases is seen when Magnetic Field i.e B is fixed.

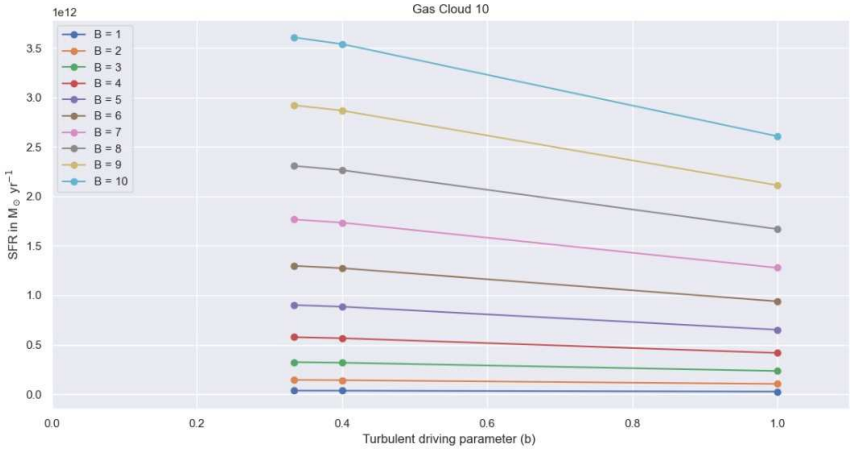

Figure 6.10: SFR vs b for Gas Cloud 10

A general decrease in SFRs as b increasing is observed , while having a little varied convergence especially before $b = 0.4$, as Magnetic Field i.e B is fixed.

7 Discussion and Conclusion

We examined the role of magnetic field $\boldsymbol{B}$ and turbulence driving parameter $\boldsymbol{b}$ in determining SFR in $\mathbf{10}$ randomly chosen SFC-GMCs from Milky Way. We have developed mathematical model of SFR and comprehensive set of numerical simulations, with the help of observational data of galactic cores. Comparing the results of two parameters, the conclusion from this study is that both $\boldsymbol{b}$ and $\boldsymbol{B}$ seem to play their part in determining SFR but the degree of compression initiated by $\boldsymbol{b}$ have solid impact on SFR causing vibration more than $\mathbf{3-4}$ significant degrees, ([132]) while the magnetic field represents the variation in SFR by merely factor of $\mathbf{1-2}$. ([102]).

In case of SFR vs. $\boldsymbol{B}$ plot that is Fig $\mathbf{5.1}$, turbulent driving parameter is taken constant (at natural mixing $\boldsymbol{b} \sim \mathbf{0.4}$). In Cloud $\mathbf{7}$, the general trend seen is decrease in SFR as $\boldsymbol{B}$ increases , while all other cloud shows increase in SFR as $\boldsymbol{B}$ increases. In case of Cloud $\mathbf{7}$, magnetic field reduces the fragmentation, subsequently providing stabilization to cloud, due to which time to reach star formation efficiency increases, leading to further increase decrease in SFRs. ([118]).Whereas in the case of all other clouds we can reason that here gravitational pressure dominates magnetic pressure, which prompts increase in SFRs and we get an expected trend.([133])

In Fig $\mathbf{6.(2,3,4,5,6,7,8,9,9,10)}$, our simulation results seem to show general trends of SFR vs $\boldsymbol{b}$ with fixed $\boldsymbol{B}$(fixed at $[\mathbf{1,10}]\,\boldsymbol{\mu G}$)
In the plots of Gas Cloud $\mathbf{1,2,3,5,6,7,9}$, shows general increase in SFRs as $\boldsymbol{b}$ increases, the reason of which is because of the fact that while moving from solenoidal mode to compressive mode, the densities of the core increases which leads to increase in SFRs.([134], [135], [136]). In this case, as magnetic field $\boldsymbol{B}$, the slope of graph SFR vs. $\boldsymbol{b}$ decreases and then graphs goes on converging.

Whereas the gas clouds $\mathbf{4,8,10}$ show general decrease in SFRs as $\boldsymbol{b}$ goes on increasing. In these exceptions, cloud $\mathbf{4}$ and $\mathbf{8}$ shows similar converging trend, while cloud $\mathbf{10}$ has little varied convergence especially before the $\boldsymbol{b} = \mathbf{0.4}$. In cloud $\mathbf{10}$, when $\boldsymbol{b} < 4$, SFR increases slightly and then goes on converging, whereas in cloud $\mathbf{4}$ and $\mathbf{8}$ it decreases slightly before $\mathbf{0.4}$ and then goes on converging. In these clouds, as magnetic field $\boldsymbol{B}$ increases the slope of graph SFR vs. $\boldsymbol{b}$ increases. The reason for this unexpected decrease in SFR may sprout from protostellar outflows([137]), expulsion of magnetic flux, or radiative feedback etc. ([138], [139], [140]) To give a proper reason as to their decrease in SFRs, we need to do more data analysis on larger set of SFC-GMCs than just $\mathbf{10}$, and take into consideration non-ideal effects where relevant. From the parameters, that govern SFR, we need to take $\boldsymbol{\mathcal{M}}$, and there is a possibility then as to narrow down the set of possibilities that may govern the seen trend of SFRs in cloud $\mathbf{4,8,10}$

8 Future Scope

The Paper talks about the development and the process of MHD and SFR in the terms of field lines. But the future scope is the secondary approach to understand the MHD just after the formation of the star, and recalculating the possible outcomes from the coronal mass ejection of the star. The Literature Reviews (such as [141] [142] [143]) in this context boldly claim about the tubular approach of solving flares and resolving the parameters that influences the MHD of the Stars During the studies of the MHD Equations, we thought of what other parameters might influence the MHD and among them the Flares and Solar Coronal effects tops the listing and although many terminal papers has been published individually on solar corona. But the factor of including MHD Influences to understand the models in this point of view is a scope of future development of this field.

On Monitoring the behaviours of the SFR-β Graphs and Analysis of the previous approach models in order to solve this statement, it has been observed a vivid approach of understanding solar flares in terms of tubular flow and planar flow. Thus, One-Dimensional Streak Line Flow has been chosen as the elementary analysis of the fluid particular behaviour of the flares to contribute into Coronal Effects and ultimately resulting into MHD Contribution. The team holds a small part of progress on this approach and is open to access if claimed. The team eventually wants to meet the minute criteria to study the basics of the origin of MHD affected due to the turbulence caused by the interpretation of Coronal Effects and Solar flare. It is also evident that we are open to work with the other teams who claims to work on this field!

APPENDIX

Following are the Python Code used for getting the value of SFR for B=10 and b = 0.4 :
Code to give value of SFR for a given set of input

```
import numpy as np
import math

import sympy as sy


def Rho(B,v_a):

    return (B**2)/(4*np.pi*v_a)

RHO = np.frompyfunc(Rho,2,1)

B = np.array([10,10,10,10,10,10,10,10,10,10])

v_a = np.array([5.4,3.825,2.67,1.74,4.685,1.69,3.44,1.875,2.795,2.765])

a = RHO(B,v_a)

rho = np.array(a.tolist())


def So(rho,C_s,B):

    M = 10

    b = 0.4

    pi = np.pi

    k = math.log(1 + ((b**2)*(M**2)*(rho*(C_s)**2)/((rho*(C_s)**2)+ (B**2/8*pi))))


    return -1*(0.5)*k


def SFR(rho,S_crit,B,C_s,So,t_ff,M_c,rho_o):

    G = 6.67 * 10**(-11)
    M = 10
    pi = np.pi
    b = 0.4

    k = math.log(1 + ((b**2)*(M**2)*(rho*(C_s)**2)/((rho*(C_s)**2)+ (B**2/8*pi))))

    a = ((3*pi/(32*G*rho_o))**(0.5))*(1/t_ff)*(rho/rho_o)*(1/math.sqrt(2*pi*k))

    x = (pi*k/2)**(0.5)

    y = math.erf((S_crit-So)/math.sqrt(2*k))

    return (-0.5*(a*x*y - a*x)*M_c)/((3*pi/32*G)**(0.5))
# This function was obtained after doing the integration

calSFR = np.frompyfunc(SFR,8,1)

S_o = np.frompyfunc(So,3,1)

rho_o = np.array([63.1,161,223,218,151,113,73.6,188,87.1,234])

C_s = np.array([1.088,0.765,0.534,0.348,0.937,0.338,0.688,0.375,0.559,0.553])

S_crit = np.array([2.9386,0.6312,0.3079,-0.5833,1.7157,0.3194,1.943,-0.3736,1.117,-1.195])

t_ff = np.array([9.32,7.41,4.66,5.26,5.61,5.22,7.97,5.62,5.73,4.45])

M_c = np.array([9.47*10**5,8.49*10**6,2.97*10**6,3.51*10**6,
2.33*10**6,7.69*10**5,9.33*10*5,3.43*10**6,1.24*10**6,2.69*10**6])
```

```
#Above values were taken from the data set
arr = S_o(rho,C_s,B)
So = np.array(arr.tolist())

print("For B=10 ,b = 0.4 SFR:", calSFR(rho,S_crit,B,C_s,So,t_ff,M_c,rho_o).tolist())
```

References

[1] Telemachos Ch. Mouschovias. *Cosmic Magnetism and the Basic Physics of the Early Stages of Star Formation*, pages 61–122. Springer Netherlands, Dordrecht, 1991. ISBN 978-94-011-3642-6. doi: 10.1007/978-94-011-3642-6_3. URL https://doi.org/10.1007/978-94-011-3642-6_3.

[2] Telemachos Ch. Mouschovias and Glenn E. Ciolek. *Magnetic Fields and Star Formation: A Theory Reaching Adulthood*, pages 305–340. Springer Netherlands, Dordrecht, 1999. ISBN 978-94-011-4509-1. doi: 10.1007/978-94-011-4509-1_9. URL https://doi.org/10.1007/978-94-011-4509-1_9.

[3] Mordecai-Mark Mac Low and Ralf S. Klessen. Control of star formation by supersonic turbulence. *Rev. Mod. Phys.*, 76:125–194, Jan 2004. doi: 10.1103/RevModPhys.76.125. URL https://link.aps.org/doi/10.1103/RevModPhys.76.125.

[4] Christopher F. McKee and Eve C. Ostriker. Theory of star formation. *Annual Review of Astronomy and Astrophysics*, 45(1):565–687, 2007. doi: 10.1146/annurev.astro.45.051806.110602. URL https://doi.org/10.1146/annurev.astro.45.051806.110602.

[5] Paolo Padoan and Ake Nordlund. A super-alfvenic model of dark clouds. *The Astrophysical Journal*, 526(1):279–294, nov 1999. doi: 10.1086/307956. URL https://doi.org/10.1086/307956.

[6] Fumitaka Nakamura and Zhi-Yun Li. Magnetically regulated star formation in three dimensions: The case of the taurus molecular cloud complex. *The Astrophysical Journal*, 687 (1):354–375, nov 2008. doi: 10.1086/591641. URL https://doi.org/10.1086/591641.

[7] Fumitaka Nakamura and Zhi-Yun Li. Clustered star formation in magnetic clouds: Properties of dense cores formed in outflow-driven turbulence. *The Astrophysical Journal*, 740(1):36, sep 2011. doi: 10.1088/0004-637x/740/1/36. URL https://doi.org/10.1088/0004-637x/740/1/36.

[8] Takahiro Kudoh and Shantanu Basu. Three-dimensional simulation of magnetized cloud fragmentation induced by nonlinear flows and ambipolar diffusion. *The Astrophysical Journal*, 679(2):L97–L100, may 2008. doi: 10.1086/589618. URL https://doi.org/10.1086/589618.

[9] Enrique Vázquez-Semadeni, Robi Banerjee, Gilberto C. Gómez, Patrick Hennebelle, Dennis Duffin, and Ralf S. Klessen. Molecular cloud evolution – IV. Magnetic fields, ambipolar diffusion and the star formation efficiency. *Monthly Notices of the Royal Astronomical Society*, 414(3):2511–2527, 06 2011. ISSN 0035-8711. doi: 10.1111/j.1365-2966.2011.18569.x. URL https://doi.org/10.1111/j.1365-2966.2011.18569.x.

[10] David A. Tilley and Ralph E. Pudritz. The formation of star clusters – II. 3D simulations of magnetohydrodynamic turbulence in molecular clouds. *Monthly Notices of the Royal Astronomical Society*, 382(1):73–94, 10 2007. ISSN 0035-8711. doi: 10.1111/j.1365-2966.2007.12371.x. URL https://doi.org/10.1111/j.1365-2966.2007.12371.x.

[11] Richard M. Crutcher. Magnetic fields in molecular clouds. *Annual Review of Astronomy and Astrophysics*, 50(1):29–63, 2012. doi: 10.1146/annurev-astro-081811-125514. URL https://doi.org/10.1146/annurev-astro-081811-125514.

[12] Patrick Hennebelle and Shu-ichiro Inutsuka. The role of magnetic field in molecular cloud formation and evolution. *Frontiers in Astronomy and Space Sciences*, 6:5, 2019. ISSN 2296-987X. doi: 10.3389/fspas.2019.00005. URL https://www.frontiersin.org/article/10.3389/fspas.2019.00005.

[13] H. C. Spruit. Essential Magnetohydrodynamics for Astrophysics. *arXiv e-prints*, art. arXiv:1301.5572, January 2013. URL https://arxiv.org/abs/1301.5572v3.

[14] P. A. Davidson. *An Introduction to Magnetohydrodynamics*. Cambridge Texts in Applied Mathematics. Cambridge University Press, 2001. doi: 10.1017/CBO9780511626333.

[15] J. D. Anderson. *Governing Equations of Fluid Dynamics*, pages 15–51. Springer Berlin Heidelberg, Berlin, Heidelberg, 1992. ISBN 978-3-662-11350-9. doi: 10.1007/978-3-662-11350-9_2. URL https://doi.org/10.1007/978-3-662-11350-9_2.

[16] Arnab Rai Choudhuri. *The Physics of Fluids and Plasmas: An Introduction for Astrophysicists*. Cambridge University Press, 1998. doi: 10.1017/CBO9781139171069.

[17] J.D. Anderson. *Fundamentals of Aerodynamics*. McGraw-Hill Education, 2010. ISBN 9780073398105. URL https://books.google.co.in/books?id=xwY8PgAACAAJ.

[18] H.W. Liepmann and A. Roshko. *Elements of Gas Dynamics*. Dover Books on Aeronautical Engineering. Dover Publications, 2013. ISBN 9780486316857. URL https://books.google.co.in/books?id=IWrCAgAAQBAJ.

[19] J.D. Anderson. *Modern Compressible Flow: With Historical Perspective*. Aeronautical and Aerospace Engineering Series. McGraw-Hill Education, 2003. ISBN 9780072424430. URL https://books.google.co.in/books?id=woeqa4-a5EgC.

[20] Francis F. Chen. *Waves in Plasmas*, pages 75–144. Springer International Publishing, Cham, 2016. ISBN 978-3-319-22309-4. doi: 10.1007/978-3-319-22309-4_4. URL https://doi.org/10.1007/978-3-319-22309-4_4.

[21] R.M. Kulsrud. *Plasma Physics for Astrophysics*. Princeton University Press, 2020. ISBN 9780691213354. URL https://books.google.co.in/books?id=DubaDwAAQBAJ.

[22] P.H. Roberts. *An Introduction to Magnetohydrodynamics*. UMI, 1987. ISBN 9780317086690. URL https://books.google.co.in/books?id=6KKnAAAACAAJ.

[23] S. Chandrasekhar and E. Fermi. Magnetic Fields in Spiral Arms. , 118:113, July 1953. doi: 10.1086/145731.

[24] S. Chandrasekhar and E. Fermi. Problems of Gravitational Stability in the Presence of a Magnetic Field. , 118:116, July 1953. doi: 10.1086/145732.

[25] L. Mestel and Jr Spitzer, L. Star Formation in Magnetic Dust Clouds. *Monthly Notices of the Royal Astronomical Society*, 116(5):503–514, 10 1956. ISSN 0035-8711. doi: 10.1093/mnras/116.5.503. URL https://doi.org/10.1093/mnras/116.5.503.

[26] Christopher F. McKee and Ellen G. Zweibel. On the Virial Theorem for Turbulent Molecular Clouds. , 399:551, November 1992. doi: 10.1086/171946.

[27] Mark R. Krumholz and Christoph Federrath. The role of magnetic fields in setting the star formation rate and the initial mass function. *Frontiers in Astronomy and Space Sciences*, 6: 7, 2019. ISSN 2296-987X. doi: 10.3389/fspas.2019.00007. URL https://www.frontiersin.org/article/10.3389/fspas.2019.00007.

[28] Laura M. Fissel and BLAST-Pol Collaboration. Probing the Role of Magnetic Fields in Star Formation with BLAST-Pol. In *American Astronomical Society Meeting Abstracts #219*, volume 219 of *American Astronomical Society Meeting Abstracts*, page 220.02, January 2012.

[29] T. Ch. Mouschovias and Jr. Spitzer, L. Note on the collapse of magnetic interstellar clouds. , 210:326, December 1976. doi: 10.1086/154835.

[30] T. Nakano and T. Nakamura. Gravitational Instability of Magnetized Gaseous Disks 6. , 30: 671–680, January 1978.

[31] Kohji Tomisaka, Satoru Ikeuchi, and Takashi Nakamura. Equilibria and Evolutions of Magnetized, Rotating, Isothermal Clouds. II. The Extreme Case: Nonrotating Clouds. , 335: 239, December 1988. doi: 10.1086/166923.

[32] Frank H. Shu, Fred C. Adams, and Susana Lizano. Star formation in molecular clouds: Observation and theory. *Annual Review of Astronomy and Astrophysics*, 25(1):23–81, 1987. doi: 10.1146/annurev.aa.25.090187.000323. URL https://doi.org/10.1146/annurev.aa.25.090187.000323.

[33] E. V. Paleologou and T. Ch. Mouschovias. The magnetic flux problem and ambipolar diffusion during star formation - One-dimensional collapse. I - Formulation of the problem and method of solution. , 275:838–857, December 1983. doi: 10.1086/161578.

[34] Christopher F. McKee, Pak Shing Li, and Richard I. Klein. SUB-ALFVéNIC NON-IDEAL MHD TURBULENCE SIMULATIONS WITH AMBIPOLAR DIFFUSION. II. COMPARISON WITH OBSERVATION, CLUMP PROPERTIES, AND SCALING TO PHYSICAL UNITS. *The Astrophysical Journal*, 720(2):1612–1634, aug 2010. doi: 10.1088/0004-637x/720/2/1612. URL https://doi.org/10.1088/0004-637x/720/2/1612.

[35] Rudolf Kippenhahn, Alfred Weigert, and Achim Weiss. *The Onset of Star Formation*, pages 299–309. Springer Berlin Heidelberg, Berlin, Heidelberg, 2012. ISBN 978-3-642-30304-3. doi: 10.1007/978-3-642-30304-3_26. URL https://doi.org/10.1007/978-3-642-30304-3_26.

[36] J. E. Dyson and D. A. Williams. *Star Formation and Star-forming regions*. CRC Press, 1997. doi: 10.1201/9780585368115.

[37] Susanne Höfner. Gravitational collapse: Jeans criterion and free fall time. 2010. URL https://www.astro.uu.se/~hoefner/astro/teach/apd_files/apd_collapse.pdf.

[38] F. Hoyle. On the Fragmentation of Gas Clouds Into Galaxies and Stars. , 118:513, November 1953. doi: 10.1086/145780.

[39] M. J. Rees. Opacity-Limited Hierarchical Fragmentation and the Masses of Protostars. *Monthly Notices of the Royal Astronomical Society*, 176(3):483–486, 09 1976. ISSN 0035-8711. doi: 10.1093/mnras/176.3.483. URL https://doi.org/10.1093/mnras/176.3.483.

[40] Steven W. Stahler and Francesco Palla. *The Formation of Stars*. 2004.

[41] Mark R. Krumholz, Eduardo Telles, Renato Dupke, and Daniela Lazzaro. Star formation in molecular clouds. 2011. doi: 10.1063/1.3636038. URL http://dx.doi.org/10.1063/1.3636038.

[42] Katia M. Ferrière. The interstellar environment of our galaxy. *Rev. Mod. Phys.*, 73: 1031–1066, Dec 2001. doi: 10.1103/RevModPhys.73.1031. URL https://link.aps.org/doi/10.1103/RevModPhys.73.1031.

[43] Bruce G. Elmegreen and John Scalo. Interstellar turbulence i: Observations and processes. *Annual Review of Astronomy and Astrophysics*, 42(1):211–273, 2004. doi: 10.1146/annurev.astro.41.011802.094859. URL https://doi.org/10.1146/annurev.astro.41.011802.094859.

[44] P Padoan, C Federrath, G Chabrier, NJ Evans, D Johnstone, JK Jørgensen, CF McKee, Å Nordlund, H Beuther, RS Klessen, et al. Protostars and planets vi. *preprint*, 2014.

[45] Uriel Frisch and Andre Nikolaevich Kolmogorov. *Turbulence: the legacy of AN Kolmogorov*. Cambridge university press, 1995.

[46] Dieter Biskamp. *Magnetohydrodynamic Turbulence*. Cambridge University Press, 2003. doi: 10.1017/CBO9780511535222.

[47] E. Falgarone and T. Passot. *Turbulence and Magnetic Fields in Astrophysics*. Lecture Notes in Physics. Springer Berlin Heidelberg, 2003. ISBN 9783540002741. URL https://books.google.co.in/books?id=NPSu2753WUkC.

[48] Alexander A. Schekochihin and Steven C. Cowley. *Turbulence and Magnetic Fields in Astrophysical Plasmas*, pages 85–115. Springer Netherlands, Dordrecht, 2007. ISBN 978-1-4020-4833-3. doi: 10.1007/978-1-4020-4833-3_6. URL https://doi.org/10.1007/978-1-4020-4833-3_6.

[49] Mark R. Krumholz. Notes on Star Formation. *arXiv e-prints*, art. arXiv:1511.03457, November 2015.

[50] E. Hecht. *Optics*. Pearson education. Addison Wesley, 2002. ISBN 9780321188786. URL https://books.google.co.in/books?id=T3ofAQAAMAAJ.

[51] L. Woltjer. A theorem on force-free magnetic fields. *Proceedings of the National Academy of Sciences*, 44(6):489–491, 1958. ISSN 0027-8424. doi: 10.1073/pnas.44.6.489. URL https://www.pnas.org/content/44/6/489.

[52] A. Kolmogorov. The Local Structure of Turbulence in Incompressible Viscous Fluid for Very Large Reynolds' Numbers. *Akademiia Nauk SSSR Doklady*, 30:301–305, 1941.

[53] Andrej Nikolaevich Kolmogorov. On the degeneration of isotropic turbulence in an incompressible viscous fluid. *Dokl. Akad. Nauk SSSR*, 31:319–323, 1941. URL http://cds.cern.ch/record/739747.

[54] Lewis Fry Richardson and Peter Lynch. *Weather Prediction by Numerical Process*. Cambridge Mathematical Library. Cambridge University Press, 2 edition, 2007. doi: 10.1017/CBO9780511618291.

[55] U. Frisch and J. Bec. *Burgulence*, pages 341–383. Springer Berlin Heidelberg, Berlin, Heidelberg, 2001. ISBN 978-3-540-45674-2. doi: 10.1007/3-540-45674-0_7. URL https://doi.org/10.1007/3-540-45674-0_7.

[56] P. S. Iroshnikov. Turbulence of a Conducting Fluid in a Strong Magnetic Field. , 7:566, February 1964.

[57] Robert H. Kraichnan. Inertial-Range Spectrum of Hydromagnetic Turbulence. *Physics of Fluids*, 8(7):1385–1387, July 1965. doi: 10.1063/1.1761412.

[58] J. V. Shebalin, W. H. Matthaeus, and D. Montgomery. Anisotropy in MHD turbulence due to a mean magnetic field. *Journal of Plasma Physics*, 29(3):525–547, June 1983. doi: 10.1017/S0022377800000933.

[59] R. Grappin. Onset and decay of two-dimensional magnetohydrodynamic turbulence with velocity-magnetic field correlation. *Physics of Fluids*, 29(8):2433–2443, August 1986. doi: 10.1063/1.865536.

[60] S. Sridhar and P. Goldreich. Toward a Theory of Interstellar Turbulence. I. Weak Alfvenic Turbulence. , 432:612, September 1994. doi: 10.1086/174600.

[61] P. Goldreich and S. Sridhar. Toward a Theory of Interstellar Turbulence. II. Strong Alfvenic Turbulence. , 438:763, January 1995. doi: 10.1086/175121.

[62] P. Goldreich and S. Sridhar. Magnetohydrodynamic turbulence revisited. *The Astrophysical Journal*, 485(2):680–688, aug 1997. doi: 10.1086/304442. URL https://doi.org/10.1086/304442.

[63] K. R. Sreenivasan and R. A. Antonia. The phenomenology of small-scale turbulence. *Annual Review of Fluid Mechanics*, 29(1):435–472, 1997. doi: 10.1146/annurev.fluid.29.1.435. URL https://doi.org/10.1146/annurev.fluid.29.1.435.

[64] D. C. Lis, J. Pety, T. G. Phillips, and E. Falgarone. Statistical Properties of Line Centroid Velocities and Centroid Velocity Increments in Compressible Turbulence. , 463:623, June 1996. doi: 10.1086/177276.

[65] L.F. Burlaga. Intermittent turbulence in the solar wind. *Journal of Geophysical Research: Space Physics*, 96(A4):5847–5851, 1991. doi: https://doi.org/10.1029/91JA00087. URL https://agupubs.onlinelibrary.wiley.com/doi/abs/10.1029/91JA00087.

[66] Politano, H., Pouquet, A., and Carbone, V. Determination of anomalous exponents of structure functions in two-dimensional magnetohydrodynamic turbulence. *Europhys. Lett.*, 43(5):516–521, 1998. doi: 10.1209/epl/i1998-00391-2. URL https://doi.org/10.1209/epl/i1998-00391-2.

[67] Dieter Biskamp and Wolf-Christian Müller. Decay laws for three-dimensional magnetohydrodynamic turbulence. *Phys. Rev. Lett.*, 83:2195–2198, Sep 1999. doi: 10.1103/PhysRevLett.83.2195. URL https://link.aps.org/doi/10.1103/PhysRevLett.83.2195.

[68] Dieter Biskamp and Wolf-Christian Müller. Scaling properties of three-dimensional isotropic magnetohydrodynamic turbulence. *Physics of Plasmas*, 7(12):4889–4900, 2000. doi: 10.1063/1.1322562. URL https://doi.org/10.1063/1.1322562.

[69] A. N. Kolmogorov. A refinement of previous hypotheses concerning the local structure of turbulence in a viscous incompressible fluid at high reynolds number. *Journal of Fluid Mechanics*, 13(1):82–85, 1962. doi: 10.1017/S0022112062000518.

[70] Zhen-Su She and Emmanuel Leveque. Universal scaling laws in fully developed turbulence. *Phys. Rev. Lett.*, 72:336–339, Jan 1994. doi: 10.1103/PhysRevLett.72.336. URL https://link.aps.org/doi/10.1103/PhysRevLett.72.336.

[71] Bérengère Dubrulle. Intermittency in fully developed turbulence: Log-poisson statistics and generalized scale covariance. *Phys. Rev. Lett.*, 73:959–962, Aug 1994. doi: 10.1103/PhysRevLett.73.959. URL https://link.aps.org/doi/10.1103/PhysRevLett.73.959.

[72] Stanislav Boldyrev. Kolmogorov-burgers model for star-forming turbulence. *The Astrophysical Journal*, 569(2):841–845, apr 2002. doi: 10.1086/339403. URL https://doi.org/10.1086/339403.

[73] Philip C. Myers. *Physical Conditions in Nearby Molecular Clouds*, pages 67–96. Springer Netherlands, Dordrecht, 1999. ISBN 978-94-011-4509-1. doi: 10.1007/978-94-011-4509-1_3. URL https://doi.org/10.1007/978-94-011-4509-1_3.

[74] Christopher F. McKee. *The Dynamical Structure and Evolution of Giant Molecular Clouds*, pages 29–66. Springer Netherlands, Dordrecht, 1999. ISBN 978-94-011-4509-1. doi: 10.1007/978-94-011-4509-1_2. URL https://doi.org/10.1007/978-94-011-4509-1_2.

[75] Mordecai-Mark Mac Low. The energy dissipation rate of supersonic, magnetohydrodynamic turbulence in molecular clouds. *The Astrophysical Journal*, 524(1):169–178, oct 1999. doi: 10.1086/307784. URL https://doi.org/10.1086/307784.

[76] W. H. Matthaeus, Sean Oughton, Sanjoy Ghosh, and Murshed Hossain. Scaling of anisotropy in hydromagnetic turbulence. *Phys. Rev. Lett.*, 81:2056–2059, Sep 1998. doi: 10.1103/PhysRevLett.81.2056. URL https://link.aps.org/doi/10.1103/PhysRevLett.81.2056.

[77] Antonio C. Ting, William H. Matthaeus, and David Montgomery. Turbulent relaxation processes in magnetohydrodynamics. *The Physics of Fluids*, 29(10):3261–3274, 1986. doi: 10.1063/1.865843. URL https://aip.scitation.org/doi/abs/10.1063/1.865843.

[78] S. Ghosh, W. H. Matthaeus, and D. Montgomery. The evolution of cross helicity in driven/dissipative two-dimensional magnetohydrodynamics. *The Physics of Fluids*, 31(8): 2171–2184, 1988. doi: 10.1063/1.866617. URL https://aip.scitation.org/doi/abs/10.1063/1.866617.

[79] D. Biskamp. Response to "comment on 'on two-dimensional magnetohydrodynamic turbulence'" [phys. plasmas 9, 1484 (2002)]. *Physics of Plasmas*, 9(4):1486–1487, 2002. doi: 10.1063/1.1459065. URL https://doi.org/10.1063/1.1459065.

[80] Jason Maron and Peter Goldreich. Simulations of incompressible magnetohydrodynamic turbulence. *The Astrophysical Journal*, 554(2):1175–1196, jun 2001. doi: 10.1086/321413. URL https://doi.org/10.1086/321413.

[81] Rainer Beck. Galactic and extragalactic magnetic fields. *Space Sci. Rev.*, 99:243–260, 2001. doi: 10.1023/A:1013805401252.

[82] Frank H. Shu, Anthony Allen, Hsien Shang, Eve C. Ostriker, and Zhi-Yun Li. *Low-Mass Star Formation: Theory*, pages 193–226. Springer Netherlands, Dordrecht, 1999. ISBN 978-94-011-4509-1. doi: 10.1007/978-94-011-4509-1_6. URL https://doi.org/10.1007/978-94-011-4509-1_6.

[83] Richard M. Crutcher. Observations of magnetic fields in molecular clouds — testing star formation paradigms. *AIP Conference Proceedings*, 784(1):129–139, 2005. doi: 10.1063/1.2077177. URL https://aip.scitation.org/doi/abs/10.1063/1.2077177.

[84] C. Heiles and R. Crutcher. *Magnetic Fields in Diffuse HI and Molecular Clouds*, pages 137–182. Springer Berlin Heidelberg, Berlin, Heidelberg, 2005. ISBN 978-3-540-31396-0. doi: 10.1007/3540313966_7. URL https://doi.org/10.1007/3540313966_7.

[85] P. Goldreich and N. D. Kylafis. On mapping the magnetic field direction in molecular clouds by polarization measurements. , 243:L75–L78, January 1981. doi: 10.1086/183446.

[86] Richard Crutcher, Carl Heiles, and Thomas Troland. *Observations of Interstellar Magnetic Fields*, pages 155–181. Springer Berlin Heidelberg, Berlin, Heidelberg, 2003. ISBN 978-3-540-36238-8. doi: 10.1007/3-540-36238-X_6. URL https://doi.org/10.1007/3-540-36238-X_6.

[87] Shyam H Menon, Christoph Federrath, and Rolf Kuiper. On the turbulence driving mode of expanding Hii regions. *Monthly Notices of the Royal Astronomical Society*, 493(4): 4643–4656, 02 2020. ISSN 0035-8711. doi: 10.1093/mnras/staa580. URL https://doi.org/10.1093/mnras/staa580.

[88] C. A. Herron, C. Federrath, B. M. Gaensler, G. F. Lewis, N. M. McClure-Griffiths, and Blakesley Burkhart. Probes of turbulent driving mechanisms in molecular clouds from fluctuations in synchrotron intensity. *Monthly Notices of the Royal Astronomical Society*, 466(2):2272–2283, 12 2016. ISSN 0035-8711. doi: 10.1093/mnras/stw3319. URL https://doi.org/10.1093/mnras/stw3319.

[89] Christoph Federrath and Ralf S. Klessen. THE STAR FORMATION RATE OF TURBULENT MAGNETIZED CLOUDS: COMPARING THEORY, SIMULATIONS, AND OBSERVATIONS. *The Astrophysical Journal*, 761(2):156, dec 2012. doi: 10.1088/0004-637x/761/2/156. URL https://doi.org/10.1088/0004-637x/761/2/156.

[90] Florent Renaud, Frédéric Bournaud, Katarina Kraljic, and Pierre-Alain Duc. Starbursts triggered by intergalactic tides andinterstellar compressive turbulence. *Monthly Notices of the Royal Astronomical Society: Letters*, 442(1):L33–L37, 05 2014. ISSN 1745-3925. doi: 10.1093/mnrasl/slu050. URL https://doi.org/10.1093/mnrasl/slu050.

[91] C. Federrath, J. Roman-Duval, R. S. Klessen, W. Schmidt, and M.-M. Mac Low. Comparing the statistics of interstellar turbulence in simulations and observations. *Astronomy and Astrophysics*, 512:A81, Mar 2010. ISSN 1432-0746. doi: 10.1051/0004-6361/200912437. URL http://dx.doi.org/10.1051/0004-6361/200912437.

[92] Bastian Körtgen, Christoph Federrath, and Robi Banerjee. The driving of turbulence in simulations of molecular cloud formation and evolution. *Monthly Notices of the Royal Astronomical Society*, 472(2):2496–2503, Aug 2017. ISSN 1365-2966. doi: 10.1093/mnras/stx2208. URL http://dx.doi.org/10.1093/mnras/stx2208.

[93] Christoph Federrath, Ralf S. Klessen, and Wolfram Schmidt. The density probability distribution in compressible isothermal turbulence: Solenoidal versus compressive forcing. *The Astrophysical Journal*, 688(2):L79–L82, Oct 2008. ISSN 1538-4357. doi: 10.1086/595280. URL http://dx.doi.org/10.1086/595280.

[94] Daniel J. Price, Christoph Federrath, and Christopher M. Brunt. The Density Variance-Mach Number Relation in Supersonic, Isothermal Turbulence. , 727(1):L21, January 2011. doi: 10.1088/2041-8205/727/1/L21.

[95] L. Konstandin, P. Girichidis, C. Federrath, and R. S. Klessen. A New Density Variance-Mach Number Relation for Subsonic and Supersonic Isothermal Turbulence. , 761(2):149, December 2012. doi: 10.1088/0004-637X/761/2/149.

[96] Christoph Federrath and Supratik Banerjee. The density structure and star formation rate of non-isothermal polytropic turbulence. *Monthly Notices of the Royal Astronomical Society*, 448(4):3297–3313, 03 2015. ISSN 0035-8711. doi: 10.1093/mnras/stv180. URL https://doi.org/10.1093/mnras/stv180.

[97] C. A. Nolan, C. Federrath, and R. S. Sutherland. The density variance–Mach number relation in isothermal and non-isothermal adiabatic turbulence. *Monthly Notices of the Royal Astronomical Society*, 451(2):1380–1389, 06 2015. ISSN 0035-8711. doi: 10.1093/mnras/stv1030. URL https://doi.org/10.1093/mnras/stv1030.

[98] C. Federrath, J. M. Rathborne, S. N. Longmore, J. M. D. Kruijssen, J. Bally, Y. Contreras, R. M. Crocker, G. Garay, J. M. Jackson, L. Testi, and et al. The link between turbulence, magnetic fields, filaments, and star formation in the central molecular zone cloud g0.253+0.016. *The Astrophysical Journal*, 832(2):143, Nov 2016. ISSN 1538-4357. doi: 10.3847/0004-637x/832/2/143. URL http://dx.doi.org/10.3847/0004-637X/832/2/143.

[99] Christoph Federrath. The turbulent formation of stars. *Physics Today*, 71(6):38–42, 2018. doi: 10.1063/PT.3.3947. URL https://doi.org/10.1063/PT.3.3947.

[100] M. G. Wolfire, D. Hollenbach, C. F. McKee, A. G. G. M. Tielens, and E. L. O. Bakes. The Neutral Atomic Phases of the Interstellar Medium. , 443:152, April 1995. doi: 10.1086/175510.

[101] G. Pavlovski, M. D. Smith, and M.-M. Mac Low. Hydrodynamical simulations of the decay of high-speed molecular turbulence - ii. divergence from isothermality. *Monthly Notices of the Royal Astronomical Society*, 368(2):943–958, May 2006. ISSN 1365-2966. doi: 10.1111/j.1365-2966.2006.10172.x. URL http://dx.doi.org/10.1111/j.1365-2966.2006.10172.x.

[102] Mark R. Krumholz and Christopher F. McKee. A general theory of turbulence-regulated star formation, from spirals to ultraluminous infrared galaxies. *The Astrophysical Journal*, 630(1): 250–268, sep 2005. doi: 10.1086/431734. URL https://doi.org/10.1086/431734.

[103] D. Falceta-Gonçalves, I. Bonnell, G. Kowal, J. R. D. Lépine, and C. A. S. Braga. The onset of large-scale turbulence in the interstellar medium of spiral galaxies. *Monthly Notices of the Royal Astronomical Society*, 446(1):973–989, 11 2014. ISSN 0035-8711. doi: 10.1093/mnras/stu2127. URL https://doi.org/10.1093/mnras/stu2127.

[104] J. Alves, M. Lombardi, and C. J. Lada. *AA*, 462:L17, 2007.

[105] P. André, A. Men'shchikov, S. Bontemps, et al. *AA*, 518:L102, 2010.

[106] Enrique Vazquez-Semadeni, J Ballesteros-Paredes, and RS Klessen. A holistic scenario of turbulent molecular cloud evolution and control of the star formation efficiency: first tests. *The Astrophysical Journal Letters*, 585(2):L131, 2003.

[107] M Nicole Lemaster and James M Stone. Density probability distribution functions in supersonic hydrodynamic and mhd turbulence. *The Astrophysical Journal Letters*, 682(2): L97, 2008.

[108] W. B. Bonnor. Boyle's Law and gravitational instability. , 116:351, January 1956. doi: 10.1093/mnras/116.3.351.

[109] Enrique Vazquez-Semadeni. Hierarchical Structure in Nearly Pressureless Flows as a Consequence of Self-similar Statistics. , 423:681, March 1994. doi: 10.1086/173847.

[110] Paolo Padoan, Ake Nordlund, and Bernard J. T. Jones. The universality of the stellar initial mass function. , 288(1):145–152, June 1997. doi: 10.1093/mnras/288.1.145.

[111] John Scalo, Enrique Vazquez-Semadeni, David Chappell, and Thierry Passot. On the probability density function of galactic gas. i. numerical simulations and the significance of the polytropic index. *The Astrophysical Journal*, 504(2):835–853, sep 1998. doi: 10.1086/306099. URL https://doi.org/10.1086/306099.

[112] Paolo Padoan and Ake Nordlund. The stellar initial mass function from turbulent fragmentation. *The Astrophysical Journal*, 576(2):870–879, sep 2002. doi: 10.1086/341790. URL https://doi.org/10.1086/341790.

[113] F. Z. Molina, S. C. O. Glover, C. Federrath, and R. S. Klessen. The density variance–Mach number relation in supersonic turbulence – I. Isothermal, magnetized gas. *Monthly Notices of the Royal Astronomical Society*, 423(3):2680–2689, 06 2012. ISSN 0035-8711. doi: 10.1111/j.1365-2966.2012.21075.x. URL https://doi.org/10.1111/j.1365-2966.2012.21075.x.

[114] Christoph Federrath, Ralf S Klessen, and Wolfram Schmidt. The density probability distribution in compressible isothermal turbulence: solenoidal versus compressive forcing. *The Astrophysical Journal Letters*, 688(2):L79, 2008.

[115] Alexei G Kritsuk, Michael L Norman, Paolo Padoan, and Rick Wagner. The statistics of supersonic isothermal turbulence. *The Astrophysical Journal*, 665(1):416, 2007.

[116] Alexei G. Kritsuk, Michael L. Norman, Paolo Padoan, and Rick Wagner. The statistics of supersonic isothermal turbulence. *The Astrophysical Journal*, 665(1):416–431, aug 2007. doi: 10.1086/519443. URL https://doi.org/10.1086/519443.

[117] Mordecai-Mark Mac Low, Ralf S. Klessen, Andreas Burkert, and Michael D. Smith. Kinetic energy decay rates of supersonic and super-alfvénic turbulence in star-forming clouds. *Phys. Rev. Lett.*, 80:2754–2757, Mar 1998. doi: 10.1103/PhysRevLett.80.2754. URL https://link.aps.org/doi/10.1103/PhysRevLett.80.2754.

[118] D. Arzoumanian, Ph. André, P. Didelon, et al. *AA*, 529:L6, 2011.

[119] D Tamburro, H-W Rix, AK Leroy, M-M Mac Low, F Walter, RC Kennicutt, E Brinks, and WJG De Blok. What is driving the h i velocity dispersion? *The Astronomical Journal*, 137 (5):4424, 2009.

[120] Miguel A de Avillez and Dieter Breitschwerdt. Global dynamical evolution of the ism in star forming galaxies-i. high resolution 3d simulations: Effect of the magnetic field. *Astronomy & Astrophysics*, 436(2):585–600, 2005.

[121] J Andersen, J Bland-Hawthorn, and B Nordström. Cosmic evolution of stellar disk truncations: from z= 1 to the local universe ignacio trujillo', ruyman azzollini', judit bakos', john beckman. *The Galaxy Disk in Cosmological Context (IAU S254)*, (254):127, 2009.

[122] Chang-Goo Kim, Woong-Tae Kim, and Eve C. Ostriker. Galactic Spiral Shocks with Thermal Instability. , 681(2):1148–1162, July 2008. doi: 10.1086/588752.

[123] R. Beck, A. Brandenburg, D. Moss, A. Shukurov, and D. Sokoloff. *ARAA*, 34:155, 1996.

[124] B Zuckerman and Patrick Palmer. Radio radiation from interstellar molecules. *Annual Review of Astronomy and Astrophysics*, 12(1):279–313, 1974.

[125] Philip F Hopkins. The stellar initial mass function, core mass function and the last-crossing distribution. *Monthly Notices of the Royal Astronomical Society*, 423(3):2037–2044, 2012.

[126] Christopher D. Matzner and Christopher F. McKee. Efficiencies of low-mass star and star cluster formation. *The Astrophysical Journal*, 545(1):364–378, dec 2000. doi: 10.1086/317785. URL https://doi.org/10.1086/317785.

[127] Simon C. O. Glover and Mordecai-Mark Mac Low. Simulating the Formation of Molecular Clouds. I. Slow Formation by Gravitational Collapse from Static Initial Conditions. , 169(2): 239–268, April 2007. doi: 10.1086/512238.

[128] Knut Waagan, Christoph Federrath, and Christian Klingenberg. A robust numerical scheme for highly compressible magnetohydrodynamics: nonlinear stability, implementation and tests. 2011. doi: 10.1016/j.jcp.2011.01.026.

[129] Eve J. Lee, Marc-Antoine Miville-Deschênes, and Norman W. Murray. Observational evidence of dynamic star formation rate in milky way giant molecular clouds. *The Astrophysical Journal*, 833(2):229, dec 2016. doi: 10.3847/1538-4357/833/2/229. URL https://doi.org/10.3847/1538-4357/833/2/229.

[130] Richard M. Crutcher. Magnetic Fields in Molecular Clouds: Observations Confront Theory. , 520(2):706–713, August 1999. doi: 10.1086/307483.

[131] Richard M. Crutcher, Benjamin Wandelt, Carl Heiles, Edith Falgarone, and Thomas H. Troland. Magnetic Fields in Interstellar Clouds from Zeeman Observations: Inference of Total Field Strengths by Bayesian Analysis. , 725(1):466–479, December 2010. doi: 10.1088/0004-637X/725/1/466.

[132] F. Bouchut, C. Klingenberg, and K. Waagan. *Numer. Math.*, 108:7, 2007.

[133] J. Ballesteros-Paredes, E. Vázquez-Semadeni, A. Gazol, et al. *MNRAS*, 416:1436, 2011.

[134] H. Beuther, P. Schilke, T. K. Sridharan, et al. *AA*, 383:892, 2002.

[135] F. Bigiel, A. Leroy, F. Walter, et al. *AJ*, 136:2846, 2008.

[136] S. Bonazzola, J. Heyvaerts, E. Falgarone, M. Perault, and J. L. Puget.

[137] Ralph E. Pudritz and Tom P. Ray. The role of magnetic fields in protostellar outflows and star formation. *Frontiers in Astronomy and Space Sciences*, 6, Jul 2019. ISSN 2296-987X. doi: 10.3389/fspas.2019.00054. URL http://dx.doi.org/10.3389/fspas.2019.00054.

[138] Matthew R Bate. The importance of radiative feedback for the stellar initial mass function. *Monthly Notices of the Royal Astronomical Society*, 392(4):1363–1380, 2009.

[139] Dávid Guszejnov, Mark R Krumholz, and Philip F Hopkins. The necessity of feedback physics in setting the peak of the initial mass function. *Monthly Notices of the Royal Astronomical Society*, 458(1):673–680, 2016.

[140] P Hennebelle, B Commerçon, M Joos, RS Klessen, Mark Krumholz, JC Tan, and R Teyssier. Collapse, outflows and fragmentation of massive, turbulent and magnetized prestellar barotropic cores. *Astronomy & Astrophysics*, 528.

[141] Nastaran Farhang, Hossein Safari, and Michael S Wheatland. Principle of minimum energy in magnetic reconnection in a self-organized critical model for solar flares. *The Astrophysical Journal*, 859(1):41, 2018.

[142] D Vassiliadis, A Anastasiadis, M Georgoulis, and L Vlahos. Derivation of solar flare cellular automata models from a subset of the magnetohydrodynamic equations. *The Astrophysical Journal Letters*, 509(1):L53, 1998.

[143] Satoshi Inoue. Magnetohydrodynamics modeling of coronal magnetic field and solar eruptions based on the photospheric magnetic field. *Progress in Earth and Planetary Science*, 3(1):1–28, 2016.